AD_____

Award Number: W81XWH-09-1-0175

TITLE: The Role of ERK1/2 in the Progression of Anti-Androgen Resistance of MtDNA Deficient Prostate Cancer

PRINCIPAL INVESTIGATOR: Cody C. Cook, B.S.

CONTRACTING ORGANIZATION: University of Arkansas for Medical Sciences
Little Rock, Arkansas 72205-7101

REPORT DATE: March 2012

TYPE OF REPORT: Annual Summary

PREPARED FOR: U.S. Army Medical Research and Materiel Command
Fort Detrick, Maryland 21702-5012

REPORT DOCUMENTATION PAGE

Form Approved
OMB No. 0704-0188

1. REPORT DATE	2. REPORT TYPE	3. DATES COVERED
March 2012	Annual Summary	15 February 2011 – 14 February 2012

4. TITLE AND SUBTITLE

The Role of ERK1/2 in the Progression of Anti-Androgen Resistance of MtDNA Deficient Prostate Cancer

5a. CONTRACT NUMBER

5b. GRANT NUMBER
W81XWH-09-1-0175

5c. PROGRAM ELEMENT NUMBER

6. AUTHOR(S)

Cody C. Cook

E-Mail: cody.cook@gmail.com

5d. PROJECT NUMBER

5e. TASK NUMBER

5f. WORK UNIT NUMBER

7. PERFORMING ORGANIZATION NAME(S) AND ADDRESS(ES)

University of Arkansas for Medical Sciences
Little Rock, Arkansas 72205-7101

8. PERFORMING ORGANIZATION REPORT NUMBER

9. SPONSORING / MONITORING AGENCY NAME(S) AND ADDRESS(ES)
U.S. Army Medical Research and Materiel Command
Fort Detrick, Maryland 21702-5012

10. SPONSOR/MONITOR'S ACRONYM(S)

11. SPONSOR/MONITOR'S REPORT NUMBER(S)

12. DISTRIBUTION / AVAILABILITY STATEMENT
Approved for Public Release; Distribution Unlimited

13. SUPPLEMENTARY NOTES

14. ABSTRACT

Characterization of the mitochondrial genomic content of normal prostatic tissue and prostate cancer tumors have revealed that the carcinogenesis of normal prostate epithelial cells to prostate cancer generates heterogeneous tumors. Within a tumor, subpopulations of cancer cells harbor mitochondria with copy numbers of the mitochondrial genome that are reduced-to-depleted, in the presence of subpopulations of cancer cells that harbor elevated copy numbers of the mitochondrial genome. In the current report, the progression of prostate cancer tumors to a high Gleason grade was noted to be associated with a reduction of the mitochondrial genome content. It is generally acknowledged that a reduction of the mitochondrial genome content in prostate cancer has biological significance, activating a mitochondrial-retrograde signal for an aggressive phenotype that includes castration resistance, defined as hormone independence and/or anti-androgen resistance. The current report describes core mechanisms in a mitochondrial-retrograde signal, denoted as a mitochondrial-generated progression signal (mitoGPS) for the progression of PCa to the castration resistant phenotype. Briefly, it was discovered that a reduction of the mitochondrial genome content generates an increase in the cellular O2 concentration, which subsequentially elevates the cellular expression of the rate-limiting enzyme of the mevalonate pathway, HMGR. The flux in the mevalonate pathway, ultimately, generated an aberrant activation of Ras-GTPases, primarily K-Ras 4A, that signal for a diverse array of cancer progression signals, such as ERK1/2 and Akt. The mitoGPS was confirmed to advance PCa to a disease of castration resistant that could be attenuated with the reconstitution of the mitochondrial genome content.

15. SUBJECT TERMS
prostate cancer, mitochondria, mitochondrial genome (mitochondrial DNA, mtDNA), HMGR-CoA Reductase, RasGTPase, K-Ras 4A, ERK1/2, Akt, castration resistance, hormone independence, anti-androgen resistance

16. SECURITY CLASSIFICATION OF:			17. LIMITATION OF ABSTRACT	18. NUMBER OF PAGES	19a. NAME OF RESPONSIBLE PERSON
					USAMRMC
a. REPORT	b. ABSTRACT	c. THIS PAGE			19b. TELEPHONE NUMBER *(include area code)*
U	U	U	UU	30	

Table of Contents

Introduction: Proposed in the prostate cancer training grant awarded in 2009 was a research project with a mission to elicit the cellular mechanisms that progress early stage prostate cancer (PCa) to a disease that is castration resistant. The phenomenon significantly impacts society, as the second leading cause of cancer mortality of US men. It is important to note that PCa is an ageing disorder that exhibits classical signs of mitochondrial dysfunction. Recent advances in the ability to quantify the mitochondrial genome content of single cells have allowed for the discovery that the carcinogenesis of normal prostate epithelial cells to cancer cells occurs with a dysregulation of the mitochondrial genome content. Within a tumor, subpopulations of cancer cells harbor mitochondria with copy numbers of the mitochondrial genome that are reduced-to-depleted, in the presence of subpopulations of cancer cells that harbor elevated copy numbers of the mitochondrial genome. In the current report, the progression of PCa tumors to a high Gleason grade was noted to be associated with a reduction of the mitochondrial genome content. It is generally acknowledged that a reduction of the mitochondrial genome content in PCa is biological significant, activating a mitochondrial-retrograde signal for an aggressive phenotype that includes castration resistance, defined as hormone independence and/or anti-androgen resistance (AAR). Prior to the training award, no study had elicited a coherent set of components that could transduce a reduction in the mitochondrial genome content into the constitutive and concurrent activation of a diverse array of nuclear-encoded signals that progress PCa to an inevitable deadly disease. To this end, the proposed project included the establishment of a research environment for the grant's PI (Cody Cook, MD/PhD candidate) to train in the field of PCa; the design and conductance of a research project to address the phenomenon of mitochondrial genomic depletion in the progression of PCa to CR phenotype; and, the presentation and publication of the accomplishments generated from the training award in multiple venues.

Scientific Hypothesis Tested: *The reduction of the mitochondrial genome content (respiration) in PCa activates a (reversible) metabolic–to–proto-oncogenic signal that progresses the cancer to a castration resistant and, thus, a inevitably deadly disease (see Hypothetic Figure).*

Hypothetic Figure:

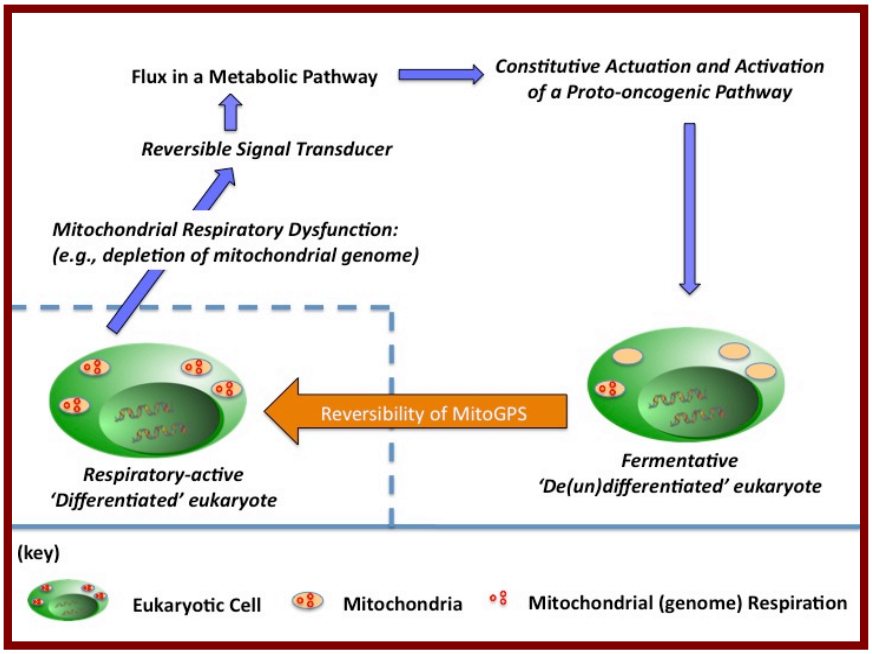

BODY: The following two scientific aims were proposed in the original Statement of Work for the prostate cancer training award.

SCIENTIFIC AIM ONE: **Characterization of the molecular activity of ERK1/2 in human prostate cell (PCa) lines reduced or depleted in mitochondrial DNA (mtDNA).**

SCIENTIFIC AIM TWO: **Investigation of the biological impact of a constitutive ERK1/2 signal on the progression of anti-androgen resistance in human PCa cell lines reduced or depleted in mtDNA.**

The progress that was accomplished for each aim is individually discussed in detail below. Most of the results were published in the report of Cook et al. (1). The philosophy behind the science was expanded upon and submitted as a review in Cook and Higuchi et al. (2). In the discussion of the specific aims, figures from Cook et al. will be referenced as 'see **Figure in Cook et al., attached document**.' Additional figures not published in Cook et al. are referenced in the discussion as 'see **Figure I in appendix**' and are attached with figure legends in the appendix section that includes a copy of Cook et al. and Cook and Higuchi et al..

It is important to note that K-Ras siRNA was utilized in place of the ERK siRNA that was purposed in the original Statement of Work, due to the better efficiency of inhibiting the mitoGPS with Ras siRNA. It is reasonable to propose that the K-Ras siRNA was more efficient due to the ability to attenuate ERK and additional effectors of the Ras with the direct silencing of the Ras-GTPase. The one task left accomplished was the electrophorectic mobility shift assays (EMSA) that were purposed to identify the transcription factor(s) downstream of phospho-ERK that repress AR expression in the PCA depleted of the mitochondrial genome. We are continuing the optimization of these experiments to address the technical aspects of the procedure.

Overall, the specific aims were clearly accomplished and expanded upon with additional scientific aims that enabled for the elicitation of a coherent set of components that integrate into a **mitochondrial-generated progression signal (mitoGPS)** that transforms the early, i.e., castration sensitive, stages of PCa into a disease that is castration resistant. The aims also enabled for the identification of biomarkers, and cell properties that warrant a continuation of research to translate the basic science, revealed with the support of the prostate cancer training award, into clinical strategies to attenuate the progression of cancers, and the viability of the inevitably fatal, CR PCa which persists in the face of the current therapeutic strategies.

AIM ONE: **Characterization of the molecular activity of ERK1/2 in human prostate cell (PCa) lines reduced or depleted in mitochondrial DNA (mtDNA).**

I(A). An evaluation of the mitochondrial genome content in PCa tumors of low Gleason grades and high Gleason grades, in addition to, adjunct normal prostate epithelial cells: As a corresponding study to Mizumachi et al. (3), in *Annual Year II* experiments were conducted to evaluate the copy number of the mitochondrial genome content within single cancerous cells isolated from human PCa tumors of a high grade (Gleason grade 8 and 9) and low grade (Gleason grade 6 and 7), in addition to, adjunct-normal epithelial cells isolated from low grade tumors. Adjunct normal epithelial cells were not present in high grade PCa tumors. Pathologist verified single cells in the prostate biopsies as cancer or normal prostate epithelium, and then the cells were individually isolated by laser microdissection. Single cells were digested into total-DNA lysates that were subjected to quantitative real time (QRT)-PCR analysis. The copy number of the (mitochondrial-encoded) ND1 gene in the DNA lysate was evaluated to determine the total-copy number of the mitochondrial genome in a single cell. The copy number of the mitochondrial genome was diminished in cancer cells that were isolated from tumors of a high grade in comparison to low grade tumors (see **Figure 1A in Cook et al., attached document**). Interestingly, cancer cells in low grade tumors harbored elevated copy numbers in comparison to adjunct normal prostate epithelial cells (see **Figure I in appendix**).

I(B). An evaluation of the mitochondrial genome content within classical cell lines which model the progression of castration-sensitive PCa to a CR phenotype: To verify the mitochondrial genomic analysis of human PCa tumors in the process of progression towards castration resistant, in *Annual Year II* experiments were conducted to evaluate the copy number of the mitochondrial genome content in classical cell lines that were derived from humans, including normal prostate epithelial cells (PrEC), early stage PCa (LNCaP), and an array of CR PCa (C4-2, PC-3 and DU-145).

LNCaP is a human PCa cell line that was established from a metastatic (supraclavicular lymph node) lesion of PCa in a patient, and the cell line is a phenotype that represents early, castration-sensitive, stages of PCa (4). C4-2 was derived from a mouse that modeled the progression of early stage PCa to an advanced (castration resistant, CR) phenotype (5). Briefly, mice inoculated with LNCaP were physically castrated after the formation of primary tumors. The tumors of LNCaP, initially, receded as a response to the androgen deprivation therapy (ADT). Tumors were found to reoccur in the bones of castrated mice, and the CR PCa was immortalized and denoted as C4-2. Additional cell lines with

a CR phenotype have been directly isolated from the metastasis of PCa to the bones and brains of patients, such as PC-3 and DU-145, respectively (6, 7).

QRT-PCR of the (mitochondrial encoded) ND1 in the denoted cell lines revealed that the copy number of the mitochondrial genome content is elevated in the early stage PCa (LNCaP) in comparison to the normal prostate epithelial cells (PrEC) (see **Figure 2 in appendix**). The copy number of the mitochondrial genome was lower in CR PCa (C4-2, PC-3 and DU-145) in comparison to LNCaP (see **Figure 1B in Cook et al., attached document**) (8). It is important to note that the mitochondrial genome content was significantly reduced in the *in vivo* progression of LNCaP to C4-2 (see **Figure 1B in Cook et al.**). The analysis of the mitochondrial genomic content in the classical PCa cell lines revealed that the shift of normal prostate epithelial cells to the early stages of PCa transiently amplifies the copy number of the mitochondrial genome. Subsequentially, the copy number is depleted as the disease progresses to CR. The transient amplification and, subsequent, depletion in the copy-number of the mitochondrial genome can be an explanation for the *Warburg Effect* that is a classical phenomenon observed in the development of cancers (9).

> **Warburg Effect:** the development of cancer is associated with a genomic insult to cellular ('mitochondrial') respiration, in addition to a flux in fermentation as the disease progresses to an advanced phenotype (9).

II. Characterization of the mitochondrial genome content within cell lines which model the depletion of the mitochondrial genome in the progression of cancers (PCa and BCa) to advanced diseases. The identification of the mitochondrial genome as a biomarker in the progression of PCa warranted the creation of cell models for the depletion of the mitochondrial genome content in the progression of PCa to a disease that is CR. Human cancers are not viable if mitochondria as a whole are removed. Mitochondria serve multiple roles for the eukaryote including ATP synthesis, redox regulation, thermogenesis, calcium regulation, and production of secondary messengers that are essential for cellular differentiation and the cell cycle (10). It is possible to generate viable cancers that are depleted of the mitochondrial genome, which are denoted as $\rho 0$. In the process of constructing a $\rho 0$ from a parental cell line, there is a potential that mutation(s) can incidentally be introduced into the nuclear genome of the $\rho 0$. The incidental mutation(s) would generate a genomic background in the $\rho 0$ that differs in comparison to the parental cell line (11). To address the potential for incidental mutations in the creation process of $\rho 0$, proper controls were established with the fusion of $\rho 0$ to cytoplast that can be derived from the parental cell line, platelets, or synaptosomes. The fusion product is the formation of a cybrid cell line that retains the nuclear-genome from the parental cell, yet harbors a mitochondrial genome content that was donated from the cytoplast (12, 13). Since the cytoplast contain no nucleus and no nuclear genome, if a phenotype generated with the depletion of the mitochondrial genome from cancer is attenuated with the reconstitution of the mitochondrial genome, the shared nuclear background of the $\rho 0$ and cybrid allows for the phenotype to be specifically attributed to the depletion of the mitochondrial genome. In other words the $\rho 0$ and cybrid confirm the phenotype is not a result of incidental nuclear mutation created in the knock out process. To this end, the following experiments were conducted to visually and quantitatively confirm the knock-out and knock-in of the mitochondrial genome content within $\rho 0$ and cybrid created from parental PCa (LNCaP) and breast cancer (BCa) (MCF-7).

PCa and BCa share similar epidemiology as the second leading causes of cancer mortality in men and women in the US (14). The cancers are the leading cancers diagnosed in the respective sexes, when basal and squamous cell skin cancers are excluded. Moreover, PCa and BCa share similar phenotypic characteristics during the progression of the cancers. The cancers originate as tumors that rely on androgen and/or endocrine sensitive signals to maintain viability, however with time the tumors can dedifferentiate into CR phenotypes that are no longer confined to hormone signals. MCF-7 is a classic human BCa cell line that is castration-sensitive, established from the metastasis (pleural effusion) of breast adenocarcinoma (15).

The $\rho 0$ of MCF-7 and LNCaP have been previously constructed and denoted as MCF$\rho 0$ and LN$\rho 0$-8, in addition to characterized as CR (16, 17). Briefly, the mitochondrial genome content was depleted from the parental cell lines by the addition of ethidium-bromide to the culture of cells. It is presumed that ethidium-bromide depletes the mitochondrial genome, preferentially over the mutation of the nuclear genome, due to the unique complementation in the charges of ethidium-bromide and mitochondria. To refine the phenotypic and molecular analysis that can be conducted with $\rho 0$, cybrid controls were constructed from the fusion of platelets to LN$\rho 0$-8 and MCF$\rho 0$ cells, and denoted as LNCyb and MCFCyb.

In *Annual Year II,* the mitochondrial genomic contents of the classic cell lines and the experimental (mtDNA-KO and mtDNA-KI) cell lines were confirmed with fluorescent *in situ* hybridization (FISH). Briefly, mitochondria were labeled with MitoTracker Red prior to fixation. Fixed cells were subjected to FISH with Alexa-488 labeled oligos (~ 600 bp) that collectively represent the entire sequence of the mitochondrial genome. Confocal microscopic images confirmed an abundance of the mtDNA probes were localized within the mitochondria of LNCaP and MCF-7, in addition to, the corresponding cybrids. No mtDNA probes were observed in the $\rho 0$ (see **Figure 1C in Cook et al., attached document**). The microscopic results were supported with the quantification of the mitochondrial genome content of single cells with QRT-PCR that was reported in *Annual Year I* (see **Figure 1D in Cook et al.**). The copy numbers obtained for the $\rho 0$ were

below detectable limits. It is important to note that the mitochondrial genome content was partially or completely restored in LNCyb and MCFCyb, respectively, to the copy number that was observed in the parental LNCaP and MCF-7.

III. The reduction-to-depletion in the copy number of the mitochondrial genome content in PCa and BCa progressively activate a Ras-to-ERK and Akt signal that is attenuated with reconstitution of the mitochondrial genome. With the confirmation of the mtDNA-KO and mtDNA-KI status of the ρ0 and the cybrid of PCa (LNCaP), models were confirmed to be proper for the elicitation of cellular mechanisms that transduce a reduction-to-depletion of the mitochondrial genome content into the progression of PCa to a disease that is CR. Previous studies of human PCa specimens have demonstrated that advanced tumors harbor canonical effectors of Ras-GTPases, such as ERK and Akt, that are constitutively activated (18, 19). Moreover, it has been shown that ERK and Akt are constitutively activated in cancers after the depletion of the mitochondrial genome (20-22). It is important to note that PCa is inherently predisposed to a deregulation in the expression and/or mutations of the phosphate and tensin homolog tumor suppressor gene. These two events can enhance the activation level of Akt (23). To identify the cellular event(s) that activates cancer signals as a response to a depletion of the mitochondrial genome, in *Annual Year I* the Ras-to-ERK/Akt pathway was characterized in early stage PCa (LNCaP) and early stage BCa (MCF-7), in comparison to corresponding ρ0 and cybrid.

Western blots of total-protein lysates with anti-phospho ERK and anti-phospho AKT confirmed that the depletion of the mitochondrial genome from LNCaP and MCF-7 enhanced the phosphorylation levels of ERK and Akt in the corresponding ρ0 (see **Figure 1E in Cook et al., attached document**). Of the two western bands that were observed in the blot of anti-phospho ERK (i.e., ERK1, p44 and ERK2, p42), ERK2 was dramatically phosphorylated in LNρ0-8 and MCFρ0 in comparison to the parental cells. Moreover, reconstitution of the mitochondrial genome to the ρ0 attenuated the phosphorylation of ERK and Akt as demonstrated in LNCyb and MCFCyb (see **Figure 1E in Cook et al.**). The results confirm that the depletion of the mitochondrial genome from PCa and BCa constitutively and concurrently activates an array of cell signals.

A canonical pathway for the aberrant activation of ERK and Akt are GTP-bound Ras-raf complexes that are formed from the interaction of GTP-bound Ras-GTPases with the Ras binding domain (RBD) of raf-1 (24-26). As small GTPases, Ras are dynamically activated and inactivated with the association of GTP or GDP, respectively. The RAS genes in human cancers often harbor oncogenic mutations that diminish the ability of Ras-GTPases to be dynamically inactivated (27). Under aerobic conditions, it is reported that oncogenic Ras can generate a flux in the fermentative pathway in respiratory-competent eukaryotic cells (28-30).

Studies of human PCa tumors have revealed that ERK and Akt are aberrantly activated as the disease progresses, yet the majority of PCa tumors are reported not to harbor RAS oncogenes (18, 19, 31). To evaluate the GTP-bound (activate) versus GDP-bound (inactive) status of Ras in cell cultures, total-protein lysates of the denoted cells were evaluated by a Ras Activation Kit. Briefly, total-protein lysates were incubated with agarose-beads bound to a glutathione S-transferase (GST) fusion protein of the human RBD of raf-1. To demonstrate the specificity of the fusion-protein for the pull-down of GTP-bound Ras, positive and negative controls were instituted with the additional supplementation of GDP or non-hydrolyzable GTPγS to lysates prior to the pull-down of GTP-bound Ras. The pre-load with GDP (negative control) induces the deactivation of Ras to the GDP-bound state and, alternatively, the pre-load with GTPγS (positive control) induces the activation of Ras to the GTP-bound state. The total-protein lysates of controls and samples were subjected to 18% SDS-PAGE, and subsequentially transferred onto membrane to be probed with anti-total-Ras.

The levels of GTP-bound Ras pulled down from lysates of early-stage PCa (LNCaP) and CR PCa (C4-2 PC-3, and DU-145) revealed the CR PCa to have lower levels of GTP-bound Ras (see **Figure 2B in Cook et al.**). The quantification of GTP-bound Ras in the CR PCa revealed the activation of the pathway to be inversely correlated with the copy number of the mitochondrial genome that were previously described (see **Figure 1C in Cook et al.**). Meanwhile, the level of GTP-bound Ras in the normal prostate epithelial cells was lower in comparison to the early stage PCa (see **Figure 2 in appendix**), though PrEC harbored a lower copy number of the mitochondrial genome than LNCaP (see **Figure 3 in appendix**). The results suggest that a tumor suppressor is silenced in the carcinogenesis of prostate tissue, predisposing the early stages of PCa to the constitutive activation of Ras-GTPases as the copy number of the mitochondrial genome content is reduced in the progression of the disease to CR.

Surprisingly, pull-downs of GTP-bound Ras were not detectable from 160 μg of lysates collected from LNCaP and MCF-7, however western blot of 160 μg of lysates collected from the corresponding ρ0 produced bands that were oversaturated (data not shown). When the probed lysates of LNρ0-8 and MCFρ0 lysates were significantly reduced to 0.5 μg or 5 μg, respectively, pull-downs of GTP-activated Ras were observed as two western bands that are characteristic for Ras-GTPases (see **Figure 2A in Cook et al.**). The experiments demonstrate that the depletion of the mitochondrial genome in PCa and BCa constitutively activates a significant quantity of Ras-GTPases.

A human cell contains three nuclear-encoded RAS genes that encode the isoforms of Ras-GTPases including H-Ras, N-Ras, and the two splice variations K-Ras 4A and K-Ras 4B (32, 33). To evaluate the isoform(s) of Ras-GPTase that are activated in PCa after the depletion of the mitochondrial genome, western blots were used to evaluate the levels of the isoforms in total-protein lysates of LNCaP and MCF-7 in comparison to the corresponding ρ0 and cybrid. The ρ0 had

elevated protein levels of K-Ras 4A in comparison to the parental and cybrid (see **Figure 3A in Cook et al.**). The evidence reveals that the depletion of the mitochondrial genome in PCa and BCa enhances the expression of K-Ras 4A, and that the aberrant expression of K-Ras 4A can be attenuated with the reconstitution of the mitochondrial genome. Further analysis of the expression of K-Ras 4A in lysates collected from CR PCa (C4-2, PC-3, DU-145, and LNρ0-8) revealed that the cellular expression of K-Ras 4A was inversely associated with the copy number of the mitochondrial genome (see **Figure 3C in Cook et al.**).

In a subsequent experiment, the relative levels of the transcripts for the Ras isoforms in LNCaP and MCF-7, in comparison to, corresponding ρ0 and cybrid models, were evaluated with reverse-transcription (RT) PCR of total-RNA lysates collected from the denoted cell lines. RT-PCR revealed that the depletion of the mitochondrial genome elevated the cellular transcript levels of K-Ras 4A. Moreover, the amplified transcript levels were attenuated with the reconstitution of the mitochondrial genome to the ρ0 in the construction of cybrids (see **Figure 3B in Cook et al.**). The observations suggest that a reduction in the copy number of the mitochondrial genome generates a flux in a Ras-to-ERK and Ras-to-Akt signal through an elevation in the transcription and activation of Ras-GPTases, predominantly K-Ras 4A.

IV. 'Proto-oncogenic' Ras is aberrantly activated when the copy number of the mitochondrial genome content is reduced in PCa and BCa. K-RAS is converted from a proto-oncogene to an oncogene in the development of a variety of cancers, such as colon cancer. Oncogenic Ras is often characterized with point mutations in codons that encode the P loop (P-L) or Switch-II (SW-II) region of the GTPase. The oncogenic mutations, ultimately, generate an intracellular accumulation of GTP-bound Ras (34). Mutations in exon one (codon 12 or 13) can encode amino-acid substitutions that render the P-L region insensitive to the activity of Ras-GTPase Activating Proteins (RasGAPs). RasGAPs catalyze the intrinsic GTPase domain of Ras and, thus, the dynamic deactivation of the molecule. The GTPase activity of Ras can be directly diminished with mutations of codon 61 in exon two. Oncogenic mutations in codon 61 encode amino-acid substitutions in the SW-II region (35).

In *Annual Year II* an evaluation of the genomic sequence of K-RAS from total-DNA lysates collected from the ρ0 of LNCaP and MCF-7 revealed codons 12, 13, and 61 of the gene to be void of oncogenic mutations (data not shown). Moreover, the characterization of K-RAS as proto-oncogenic was supported with the transfection of K-RAS siRNA into LNρ0-8. The transfection showed that the reduction of the cellular expression of K-Ras attenuated the aberrant phosphorylation of ERK and Akt (see **Figure 3D in Cook et al., attached document**). The evidence strongly suggests that the constitutive activation of K-Ras, generated with the depletion of the mitochondrial genome content in PCa and BCa, is likely of a metabolic origin rather than derived from an oncogenic mutation.

It is important to note that normal prostate epithelial cells (PrEC) harbored a low copy number of the mitochondrial genome in comparison to early stage PCa (LNCaP), yet the cellular expression of GTP-bound Ras was not amplified in PrEC as was observed in CR PCa, which were characterized with low copy numbers of the mitochondrial genome (C4-2, PC-3, DU145, and LρN0-8) (see **Figure 2 and 3 in appendix**). Regarding this paradox, reports have shown that the RasGAP activity of the DOC-2/DAB2 interactive protein (DAB2IP) is silenced in the transformation of prostate epithelial cells to PCa, predisposing the cancers to an accumulation of GTP-bound Ras (36-38). Western blot of DAB2IP in total-protein lysates collected from normal prostate epithelial cells (PrEC), early-stage PCa (LNCaP), and CR PCa (C4-2, PC-3, DU-145, and LNρ0-8) revealed that the cellular expression of DAB2IP was diminished in early stage PCa and CR PCa, in comparison to normal prostate epithelial cells (see **Figure 2C in Cook et al.**). Based on the observation that early stage PCa maintains the ability to dynamically modulate the Ras pathway (see **Figure 2A and 2B in Cook et al.**), the silencing of DAB2IP, alone, cannot explain the constitutive activation of Ras that was observed in CR PCa. It is warranted to postulate that the silencing of DAB2IP in the transformation of normal prostate epithelial cells to PCa predisposes the disease to an accumulation of GTP-bound Ras that are generated downstream to a reduction in the mitochondrial genome content.

V. The reduction-to-depletion of the mitochondrial genome content in PCa induces the mevalonate pathway to activate Ras effectors (ERK and Akt). Ras is void of a transmembrane domain. Post-translational modifications are required to enable GTP-bound Ras-Raf complexes to activate Ras effectors at the cellular membrane (39). An addition of farnesyl to the first cysteine in the C-terminus (CAAX) of Ras, i.e., prenylation, can enable the localization of Ras to the cellular membrane (40). The farnesyl moieties are derived from an intermediate of the mevalonate pathway, farnesyl pyrophosphate. Farnesyltransferase (FTase) catalytically transfers farnesyl moieties to Ras (41).

The farnesylation of Ras can be repressed with lovastatin-mediated inhibition of the HMG-CoA reductase (HMGR) enzyme, or, in other words, the metabolism of HMG-CoA to mevalonate (42). HMGR is a rate-limiting enzyme of the mevalonate pathway (43). To directly inhibit the farnesylation of Ras, farnesyltransferase inhibitors (FTIs) have been designed as peptidomimetics of the C-terminus of Ras (CAAX) (44). Specific FTIs, such as FTI-276, have been created to be selective for FTase over geranylgeranyl transferase I that is responsible for the posttranslational lipidation of CAAX proteins such as RHOA, RAC1, and CDC42 (44, 45).

In Annual Year II, confocal (z-slice) images and anti-Ras were used to probe fixed samples of early stage PCa (LNCaP), and, corresponding ρ0 and cybrid (see **Figure 4A in Cook et al., attached document**). Ras was primarily

observed to be in the cytosol of early stage PCa. Localization of Ras shifted to the cellular membrane after depletion of the mitochondrial genome content. The aberrant localization of Ras was inhibited after the addition of lovastatin to the culture of ρ0. It is important to note that the lovastatin-mediated effect on Ras was inhibited with the co-application of exogenous mevalonate (see **Figure 4B in Cook et al.**). Moreover, a corresponding western blot of total-protein lysates collected from LNρ0-8 cultured in the presence of lovastatin or FTI-276 revealed either agent could diminish the aberrant phosphorylation of Ras effectors (ERK and Akt) that were previously demonstrated to be downstream of the depletion of the mitochondrial genome content (see **Figure 4C** and **Figure 4D in Cook et al.**). The results support the postulate that a reduction in the copy number of the mitochondrial genome content generates a flux in the mevalonate pathway that induces the aberrant activation of Ras, in addition to, ERK and Akt.

The human cell regulates the activity of the mevalonate pathway with multiple feedback mechanisms to HMGR, including transcriptional and/or translational regulation, PTMs, and/or proteasomal degradation by both sterol and non-sterol products of the mevalonate pathway (46, 47). A western blot was used to evaluate the protein levels of HMGR in total-protein lysates collected from normal prostate epithelial cells (PrEC), early-stage PCa (LNCaP), and CR PCa (C4-2, PC-3, DU-145, and LNρ0-8). The cellular expression of HMGR was inversely associated with the copy number of the mitochondrial genome content (see **Figure 4F in Cook et al.**). Moreover, a western blot of total-protein lysates collected from LNCaP, and, corresponding ρ0 and cybrid models confirmed that the depletion of the mitochondria genome content elevates the cellular expression of HMGR. The phenomenon was noted to attenuate with the reconstitution of the mitochondrial genomic content (see **Figure 4E in Cook et al.**).

Interestingly, western blot of HMGR in total-protein lysates collected from LNCaP cultured in the presence of proteasomal inhibitor (ALLN) revealed that the ALLN increased the protein level of HMGR (see **Figure 5B in Cook et al.**). It is important to note that RT-PCR of the relative transcript level of HMGR in early stage PCa (LNCaP) and early stage BCa (MCF-7), in comparison to, corresponding ρ0 and cybrid suggest that the depletion of the mitochondrial genome content does not alter the cellular transcript levels of HMGR (data not shown). It is warranted to speculate that proteasomal degradation dampens the cellular expression of HMGR in the early stages of PCa, until a reduction in the mitochondrial genome content diminishes the proteosomal degradation of HMGR, subsequentially generating a flux in the mevalonate pathway that activates Ras signals to ERK and Akt.

VI. The cellular expression of HMGR and phosphorylation of ERK are amplified with the reduction-to-depletion of the mitochondrial genome content in PCa, in response to a normoxic-to-hyperoxic shift that is generated with the dysfunction of mitochondrial respiration. Recent reports have demonstrated that the exposure of cells to hypoxic conditions induces proteasomal degradation of the HMGR expressed within cells (48, 49). In Annual Year II, the level of hypoxia within cells was indirectly measured with quantification of the oxygen gas (O_2) concentration at the bottom of a 96 well OxoPlate. The O_2 concentration in cell-free media that was saturated with air was 217 μM. An inclusion of early stage PCa (LNCaP) to the OxoPlate media generated a normoxic-to-hypoxic shift that was significant in comparison to CR PCa (C4-2, PC-3, DU-145, and LNρ0-8) (see **Figure 6G in Cook et al., attached document**). In comparison to the mitochondrial genomic analysis of early stage PCa and CR PCa (see **Figure 1B in Cook et al.**), the results from the OxoPlate demonstrate that the cellular ability of PCa to induce hypoxic cultures is diminished as the copy number of the mitochondrial genome content is reduced.

It is important to note the presence of LNCaP or MCF-7 in the OxoPlate greatly reduced the O_2 concentration in media to a hypoxic state (12.3 and 4.2 μM, respectively) within an hour after the initiation of culture (see **Figure 6B and 6C in Cook et al.**). Moreover, the hypoxic-inducing ability of the parental cells was diminished with the depletion of the mitochondrial genome content (LNρ0 and MCFρ0). The hypoxic-inducing ability was restored with reconstitution of the mitochondrial genome content (LNCyb and MCFCyb) (see **Figure 6B and 6C in Cook et al.**). To confirm the evidence derived from the OxoPlate, an O_2 electrode was used to evaluate the O_2 consumption of cellular suspensions of the denoted cell lines. The cellular O_2 consumption rate of early stage PCa (LNCaP) was relatively high in comparison to cultures of CR PCa (C4-2, PC-3, DU-145, and LNρ0-8) (see **Figure 6A in Cook et al.**). The collective evidence from the O_2 electrode and OxoPlate techniques demonstrate that the mitochondrial genome content is a primary determinant of the hypoxic-inducing ability of PCa and BCa.

An analysis of normal prostate epithelial cells (PrEC) in the OxoPlate revealed that the cells have a strong hypoxic-inducing ability in comparison to early stage PCa (LNCaP) (see **Figure 4 in appendix**), which were previously denoted to harbor a higher copy number in the mitochondrial genome content (see **Figure 2 in appendix**). The observation warrants the postulate that the decrease in the hypoxic-inducing ability of PCa, in comparison to normal prostate epithelial cells, is a consequence of the diminished MRC activity that is generated from a mitochondrial genome content that is amplified or diminished but, yet, damaged in the process of carcinogenesis. Moreover, it is hypothesized that the hypoxic-inducing ability of prostate epithelial cells enables the cells to dynamically inactive the Ras-to ERK and Akt signals that are constitutively and progressively activated as the mitochondrial genomic content is depleted in the progression of the disease to the CR phenotype.

As a means to evaluate if hypoxic-to-normoxic shifts generate the constitutive activation of the Ras pathway,

hyperoxia was exogenously established in OxoPlate cultures of early stage PCa (LNCaP) with the incubation of cells in an enriched O_2 environment. The protein level of HMGR and the phosphorylation level of ERK were evaluated with western blot of total-protein lysates collected from LNCaP cultured in an atmosphere of normoxia or hyperoxia (20 % O_2, 217 µM or 30 % O_2, 310 µM). The protein level of HMGR and phosphorylated ERK were increased within 6 hours of incubation of LNCaP in a hyperoxic chamber (see **Figure 6D in Cook et al.**).

As an alternative technique to confirm that a hypoxic-to-normoxic shift aberrantly activates the Ras, the protein level of HMGR and the phosphorylation of ERK were evaluated with western blot of total-protein lysates collected from LNρ0-8 cultured in an atmosphere of normoxia (control) or hypoxia. Hypoxia was defined as 0.2% O_2, 2.1 µM, and used to induce a hyperoxic-to-normoxic shift in the ρ0. The results demonstrate that the culture of LNρ0-8 in a hypoxic culture for 6 hours diminished the protein level of HMGR and the phosphorylation of ERK (see **Figure 6E** and **Figure 6F in Cook et al.**). The experimental induction of the hyperoxic-to-normoxic shift in the ρ0 mirrors the evidence generated from the experimental induction of the normoxic-to-hyperoxic shift in the parental LNCaP (see **Figure 6D in Cook et al.**). The collective evidence supports the postulate that the cellular O_2 concentration is a physical link downstream of the reduction-to-depletion of the mitochondrial genome content that generates an aberrant activation of the mevalonate-to-Ras pathway. We denote the coherent series of events as the *mitoGPS* for the progression of PCa and BCa cancers to advanced diseases. It is important to note that the *mitoGPS* could be reversed with the reconstitution of a (donor) mitochondrial genome to ρ0.

AIM TWO: **Investigation of the biological impact of a constitutive ERK1/2 signal on the progression of anti-androgen resistance in human PCa cell lines reduced or depleted in mtDNA.**

VII. The CR phenotype is generated in response to a flux in the mitoGPS, after the depletion of the mitochondrial genome content in PCa. Over half a century ago, the Nobel laurite Charles Huggins reported that the viability of primary and metastatic PCa tumors was sensitive to the pharmacological inhibition of the hypothalamo-pituitary-gonadal axis. In other words, Huggins discovered that PCa was sensitive to the ablation of the systemic circulation of androgens (50). To this date, the pharmaceutical inhibition or anatomical inhibition of the axis has become a mainstay treatment for invasive PCa. While the tumors of patients with invasive and metastatic PCa recede with ADT, unfortunately, the majority of patients develop secondary CR tumors that are resistant to ADT (51). A similar phenomenon of resistance is often reported after the treatment of invasive and metastatic PCa with anti-androgens, such as flutamide. Flutamide is a competitive inhibitor to testosterone and dihydrotestosterone for the binding of the AR. In the treatment of invasive and metastatic PCa, the exposure to anti-androgens causes the disease to initially recede, and then the disease progress to an AAR phenotype that is inevitably fatal (14). Even though PCa can be effectively treated in the early stages, the potential for PCa to differentiate makes the disease the most deadly cancer for American men. In 2009 an estimated 27,360 men died as a consequence of an incomplete understanding of the cellular mechanisms of CR. The ability for PCa to remain viable outside the confined structure of the prostate, in addition to, the presence of blockades of the androgen to androgen-receptor, warrants the postulate that the *mitoGPS* generates the CR phenotype.

LNCaP is a classic cell line that represents the androgen sensitive phenotype of early stage PCa. In Annual Year I, an androgen dependence and sensitivity assay was used to confirm the androgen dependence of LNCaP. The culture media in the assay was charcoal stripped of androgens. Briefly, LNCaP was seeded at a concentration of 2,000 cells/well, overnight. The cells were cultured 7 days in charcoal stripped media supplemented with synthetic androgen R1881 and/or exogenous mevalonate. As a control, cells were also cultured in charcoal stripped media with no supplementation. Post-treatment, the viability of cell cultures was evaluated with the quantification of cellular proliferation from a calcein assay (see **Figure 7E in Cook et al., attached document**). Cell viability was also visually assessed with wide field (phase-contrast) microscopy (see **Figure 7A-7D in Cook et al.**). The results of the calcein assay and microscopic images demonstrate that the viability of early stage PCa (LNCaP) was enhanced when cultured in the presence of exogenous androgen. The co-treatment of mevalonate attenuated the dose-dependent effect that androgen elicited on the viability of LNCaP. Moreover, exogenous mevalonate supported the viability of LNCaP in the absence of exogenous androgen. The results demonstrate that the viability of early stage PCa can be supported by the androgen signal and/or a flux in the mevalonate pathway.

It has been previously reported that a reduction-to-depletion in the mitochondrial genomic contents of PCa progress the disease to the CR phenotype (8, 16, 52, 53). To access if the phenomenon is generated from a flux in the *mitoGPS*, the ρ0 of LNCaP (LNρ0-8) was cultured 48 hr in the absence (control) or presence of lovastatin. The cell cultures were additionally supplemented without or with mevalonate. Post-treatment, the viability of cell cultures was assessed with the quantification of cellular proliferation from a crystal violet assay. Lovastatin lowered the viability of LNρ0-8. Moreover, the effect of lovastatin was attenuated with the co-application of mevalonate, which induced a flux in the mevalonate pathway in the face of the lovastatin-induced blockade of HMGR (see **Figure 7G in Cook et al.**). In a corresponding experiment, it was noted that the cellular proliferation of LNρ0-8 was differentially sensitive to lovastatin in comparison to LNCaP and LNCyb (see **Figure 7F in Cook et al.**). The observations demonstrate that the mevalonate pathway mediates the CR phenotype of the CR PCa (LNρ0-8). The results support the postulate that depletion of the mitochondrial genomic content activates a

mitoGPS that enhances the viability of CR PCa.

VIII. Fluxes in the mevalonate pathway enhance the viability of early stage PCa (LNCaP) in mouse (xenograft) models. Early stage PCa (LNCaP) is known to gradually acquire more aggressive growth, *in vitro* and *in vivo* (289, 290). To investigate if cellular fluxes in the mevalonate pathway enhance the growth of PCa tumor, in Annual Year II, LNCaP were inoculated into athymic nude mice to evaluate the *in vivo* effect of the application (injection) of mevalonate and/or consumption of lovastatin. The natural increase in the *in vivo* growth of LNCaP tumors was observed over time (see **Figure 8A in Cook et al., attached document**). Lovastatin attenuated the progressive growth of the tumors, while a co-treatment with mevalonate inhibited the lovastatin-mediated effects. The treatment of mevalonate, alone, showed a slight but significant ability to enhance tumor growth (see **Figure 8E in Cook et al.**). The results indicate that a flux in the mevalonate pathway can enhance the *in vivo* growth of early stage PCa (LNCaP), potentially due to a silencing of RasGAPs in the transformation of prostate epithelial cells to PCa, which predisposes the cancer to autonomous growth generated from GTP-bound Ras.

IX: The expression of AR is diminished in response to a flux in the *mitoGPS* that is generated after the depletion of the mitochondrial genome content in PCa. Reports have estimated that 20-30% of the cell population in an advanced PCa tumor is characterized with an extensive loss in the cellular expression of AR (54). The AR-negative cells are biologically significant. Chin et al. demonstrated that AR-negative cells generate metastasis-related factors that promote the osteoblastic progression of PCa (55). In respect to the progression of BCa to the CR phenotype, Tseng et al. has shown that mitochondrial genomic mutations in the non-coding (D)-loop are associated with the silenced expression of the estrogen receptor and progesterone receptor in advanced BCa cell lines (53).

As a means to evaluate if the copy number of the mitochondrial genome was inversely associated with the cellular expression of AR in PCa, in *Annual Year I* total-protein lysates of LNCaP and the corresponding ρ0 were probed with anti-AR in a western blot. The cellular expression of AR was diminished in LNρ0-8 in comparison to the parental LNCaP (see **Figure 5 in appendix**). This result warrants the postulate that the mevalonate-to-Ras component of the *mitoGPS* diminishes the cellular expression of the AR in PCa that is depleted of mitochondrial genomic content. In a corresponding experiment, the cellular expression of AR was quantified for LNρ0-8 that was cultured 48 hr in the absence or under the pharmaceutical inhibition of ERK. PD98059 is a non-competitive inhibitor of MEK, the upstream activator of ERK in the Ras pathway. Total-protein lysates collected from the denoted cultures were subjected to SDS-PAGE and probed with anti-AR in a western blot. Total-protein lysates of LNCaP were evaluated as a positive control for the AR. Total-protein lysates were additionally probed with anti-phospho ERK to confirm that PD98059-induced the inhibition of ERK. The addition of PD98059 to the culture of ρ0 attenuated the phosphorylation of ERK and elevated the expression of AR (see **Figure 5 in appendix**). Similar results were observed when LNρ0-8 was cultured 48 hr in presence of GW5074 or U0126 (see **Figure 6 in appendix**). U0126 is a non-competitive inhibitor of MEK. GW5074 is a competitive inhibitor of raf-1, the upstream activator of MEK in the Ras pathway. The evidence suggests that a flux in the *mitoGPS*, as a response to a reduction-to-depletion in the copy number of the mitochondrial genomic content in PCa, can diminish the cellular expression of AR. Preliminary results suggest that the mitoGPS, in part, regulates the cellular expression of AR at the transcript level (see **Figure 7 in appendix**).

X: The AAR phenotype is generated in response to a flux in the mitoGPS that is generated after the depletion of the mitochondrial genome content in PCa. LNCaP is a classic cell line that models the anti-androgen sensitivity of early stage PCa. In *Annual Year I* the sensitivity of LNCaP to anti-androgen was confirmed with an anti-androgen sensitivity assay (see **Figure 4H**). Briefly, LNCaP was seeded at 2,000 cells/well in a 96 well plate, overnight. Cells were cultured 4 days in the absence or presence of the anti-androgen, flutamide. The viability of the cell cultures was assessed with the quantification of cellular proliferation from a calcein assay. The results demonstrate that the viability of LNCaP was decreased in the presence of flutamide and, thus, anti-androgen sensitive (see **Figure 8 in appendix**).

Previously it was noted from western blot that the cellular expression of AR was diminished in the ρ0 of early stage PCa (LNCaP) (see **Figure 5 and 6 in appendix**). Moreover, the application of PD98059, GW5074, or U0126 to cultures of LNρ0-8 could regenerate the expression of AR that was silenced with depletion of the mitochondria genome content from the parental LNCaP (see **Figure 5 and 6 in appendix**). In a corresponding experiment the viability of LNρ0-8 was evaluated with an anti-androgen assay to assess if the AAR phenotype concurrently develops with the silencing of the AR in ρ0. The results revealed that the cellular proliferation of LNρ0-8 was not significantly decreased from the exposure of the ρ0 to a concentration of flutamide that diminished the viability of the parental LNCaP (see **Figure 9 in appendix**). In a corresponding experiment the AAR phenotype of LNρ0-8 was assessed with an anti-androgen sensitive assay after 4 days of culture of the ρ0 in media that was additionally supplemented without (control) or with 40 μM PD98059. The anti-androgen sensitivity assay confirmed PD98059 attenuated the AAR phenotype of LNρ0-8 (see **Figure 9 in appendix**). The comparison of the AR expression and the anti-androgen sensitive assays of LNCaP, in addition to corresponding ρ0 and cybrid, confirm that PCa progress to an AAR phenotype in response to a depletion of the mitochondrial genome content. Experimentation with inhibitors of the Ras-to-ERK pathway demonstrate that the advanced (CR and AAR) phenotype can be derived from the constitutive activation of a *mitoGPS* that is activated in response to depletion of the mitochondrial genome content in PCa.

Key Research Accomplishments:

- The characterization of mitochondrial DNA contents of single cancer cells from human PCa tumors, of a low grade and a high grade, indicated that cancer cells from high grade tumors had a low mitochondrial genome content in comparison to low grade tumors.
- The characterization of mitochondrial DNA contents of single cancer cells from classical PCa cell lines revealed a low mitochondrial genome content in CR PCa in comparison early stage PCa.

- Experimental models for the depletion of the mitochondrial genome content (i.e., $\rho 0$) were created with the knock-out of the mitochondrial genome from early stage PCa (LNCaP) and early stage (BCA). A knock-in of the mitochondrial genome was generated from the fusion of platelets (donor mitochondria) with $\rho 0$ in the creation of cybrids.

- From the classical cell lines and experimental cell models was discovered the components of a mitochondrial-retrograde signal that progresses PCa to the CR phenotype, in response to a reduction-to-depletion of the mitochondrial genome. Briefly, as the copy number of the mitochondrial genome is reduced the, subsequent, dysfunction of the MRC was found to induce a flux in the cellular O_2 concentration that shifted cells from a hypoxic-to-normoxic state. The hypoxic-to-normoxic shift was found to be transduced into the metabolic profile of a cancer cell, at the level of the cellular expression of the rate limiting enzyme of the mevalonate pathway, HMGR. Ultimately, the reduction-to-depletion of the mitochondrial genome content was found to induce a flux in the mevalonate (HMGR) pathway, which generated the constitutive activation of proto-oncogenic Ras (predominantly, K-Ras 4A) and a diverse array of effectors of Ras, such as ERK and Akt.

Research Outcomes:

- The core results from the project were peer reviewed and published.
-

  C C Cook, A Kim, S Terao2, A Gotoh and M Higuchi. Consumption of oxygen: a mitochondrial-generated progression signal of advanced cancer. Cell Death and Disease (2012). PMID 22258408, PMCID PMC3270275

- The core results were presented in the form of a poster presentation at the Prostate Cancer Research Program IMPaCT 2011 Conference (March 9-12, 2011)
- Knowledge acquired from the training portion of the project were collected and published as a review article on the impact of the mitochondrial genome in the progression of cancers.

  CC Cook CC and M. Higuchi. The awakening of an advanced malignant cancer: An insult to the mitochondrial genome. Biochim Biophys Acta. (2011) PMID: 21920409, PMCID: PMC3269539

- A Prostate Cancer Discussion Group was instituted at UAMS to report monthly on current prostatic clinical and research projects in the state of Arkansas
- The project was the center of a thesis submitted in March 2012 as a part of the PhD requirements of the PI (Cody Cook). The thesis will be presented as a dissertation in April 2012 to fulfill the PhD requirements.

Conclusions: The discovery of the *mitoGPS* has identified a mechanism that can simultaneously induce a set of characteristics that define the advanced phenotypes of cancers, including: CR growth (8, 16, 56), resistant to apoptosis (8), glycolytic flux (148, 308), in addition to, enhanced invasion and metastasis (8, 20, 56). Mechanisms that have been identified for the *mitoGPS* are prospective (mitochondrial and nuclear encoded) markers for the selective penetrance, progression, and prognosis of PCa and BCa. Signaled by a metabolic-to-proto-oncogenic pathway, it is plausible that the *mitoGPS* is a ubiquitous (patho)physiological response to the etiology and/or progression of a broad spectrum of human diseases that are attributed to respiratory incompetent mitochondria, such as the clearly defined 'mtDNA depletion syndrome' and degenerative diseases (e.g., metabolic syndrome and diabetes) (57-60). Moreover, the identification of the complexity and the specificity of the *mitoGPS* could open the door for potential treatments to diseases that are associated with mitochondrial respiratory dysfunction, with therapies that are of restricted toxicity. The evidence obtained from the prostate cancer training award warrants further study the mechanics of the *mitoGPS*, as the outcome could enable a realistic fight against cancer, based on stalling and reversing the progression of the disease as we await the cure.

Bibliography:

1. Cook CC, Kim A, Terao S, Gotoh A, Higuchi M. Consumption of oxygen: a mitochondrial-generated progression signal of advanced cancer Cell Death and Diseases. In Press. PMCID: In Process.
2. Cook CC, Higuchi M. The awakening of an advanced malignant cancer: An insult to the mitochondrial genome. Biochim Biophys Acta. 2011.
3. Mizumachi T, Muskhelishvili L, Naito A, Furusawa J, Fan CY, Siegel ER, et al. Increased distributional variance of mitochondrial DNA content associated with prostate cancer cells as compared with normal prostate cells. Prostate. 2008;68(4):408-17. PMCID: 2268637.
4. Horoszewicz JS, Leong SS, Chu TM, Wajsman ZL, Friedman M, Papsidero L, et al. The LNCaP cell line--a new model for studies on human prostatic carcinoma. Prog Clin Biol Res. 1980;37:115-32.
5. Wu HC, Hsieh JT, Gleave ME, Brown NM, Pathak S, Chung LW. Derivation of androgen-independent human LNCaP prostatic cancer cell sublines: role of bone stromal cells. Int J Cancer. 1994;57(3):406-12.
6. Kaighn ME, Narayan KS, Ohnuki Y, Lechner JF, Jones LW. Establishment and characterization of a human prostatic carcinoma cell line (PC-3). Invest Urol. 1979;17(1):16-23.
7. Stone KR, Mickey DD, Wunderli H, Mickey GH, Paulson DF. Isolation of a human prostate carcinoma cell line (DU 145). Int J Cancer. 1978;21(3):274-81.
8. Moro L, Arbini AA, Marra E, Greco M. Mitochondrial DNA depletion reduces PARP-1 levels and promotes progression of t he neoplastic phenotype in prostate carcinoma. Cell Oncol. 2008;30(4):307-22.
9. Warburg O. On the origin of cancer cells. Science. 1956;123(3191):309-14.
10. Wallace DC. A mitochondrial paradigm of metabolic and degenerative diseases, aging, and cancer: a dawn for evolutionary medicine. Annu Rev Genet. 2005;39:359-407. PMCID: 2821041.
11. Rasmussen AK, Chatterjee A, Rasmussen LJ, Singh KK. Mitochondria-mediated nuclear mutator phenotype in Saccharomyces cerevisiae. Nucleic Acids Res. 2003;31(14):3909-17. PMCID: 165961.
12. Kulawiec M, Owens KM, Singh KK. mtDNA G10398A variant in African-American women with breast cancer provides resistance to apoptosis and promotes metastasis in mice. J Hum Genet. 2009;54(11):647-54. PMCID: 2909846.
13. Inoue K, Ito S, Takai D, Soejima A, Shisa H, LePecq JB, et al. Isolation of mitochondrial DNA-less mouse cell lines and t heir application for trapping mouse synaptosomal mitochondrial DNA with deletion mutations. J Biol Chem. 1997;272(24):15510-5.
14. American_Cancer_Society. American Cancer Society. Cancer Facts & Figures 2009. Atlanta 2009 Contract No.: Document Number|.
15. Soule HD, Vazguez J, Long A, Albert S, Brennan M. A human cell line from a pleural effusion derived from a breast carcinoma. J Natl Cancer Inst. 1973;51(5):1409-16.
16. Higuchi M, Kudo T, Suzuki S, Evans TT, Sasaki R, Wada Y, et al. Mitochondrial DNA determines androgen dependence in prostate cancer cell lines. Oncogene. 2006;25(10):1437-45. PMCID: 2215312.
17. Naito A, Carcel-Trullols J, Xie CH, Evans TT, Mizumachi T, Higuchi M. Induction of acquired resistance to antiestrogen by reversible mitochondrial DNA depletion in breast cancer cell line. Int J Cancer. 2008;122(7):1506-11. PMCID: 2293290.
18. Gioeli D, Mandell JW, Petroni GR, Frierson HF, Jr., Weber MJ. Activation of mitogen-activated protein kinase associated with prostate cancer progression. Cancer Res. 1999;59(2):279-84.
19. Malik SN, Brattain M, Ghosh PM, Troyer DA, Prihoda T, Bedolla R, et al. Immunohistochemical demonstration of phospho-Akt in high Gleason grade prostate cancer. Clin Cancer Res. 2002;8(4):1168-71.
20. Naito A, Cook CC, Mizumachi T, Wang M, Xie CH, Evans TT, et al. Progressive tumor features accompany epithelial-mesenchymal transition induced in mitochondrial DNA-depleted cells. Cancer Sci. 2008;99(8):1584-8. PMCID: 2535852.
21. Suzuki S, Naito A, Asano T, Evans TT, Reddy SA, Higuchi M. Constitutive activation of AKT pathway inhibits TNF-induced apoptosis in mitochondrial DNA-deficient human myelogenous leukemia ML-1a. Cancer Lett. 2008;268(1):31-7. PMCID: 2562876.
22. Higuchi M, Manna SK, Sasaki R, Aggarwal BB. Regulation of the activation of nuclear factor kappaB by mitochondrial respiratory function: evidence for the reactive oxygen species-dependent and -independent pathways. Antioxidants & Redox Signaling. 2002;4(6):945-55.
23. McMenamin ME, Soung P, Perera S, Kaplan I, Loda M, Sellers WR. Loss of PTEN expression in paraffin-embedded primary prostate cancer correlates with high Gleason score and advanced stage. Cancer Res. 1999;59(17):4291-6.
24. Zhang XF, Settleman J, Kyriakis JM, Takeuchi-Suzuki E, Elledge SJ, Marshall MS, et al. Normal and oncogenic p21ras proteins bind to the amino-terminal regulatory domain of c-Raf-1. Nature. 1993;364(6435):308-13.
25. Minden A, Lin A, McMahon M, Lange-Carter C, Derijard B, Davis RJ, et al. Differential activation of ERK and JNK mitogen-activated protein kinases by Raf-1 and MEKK. Science. 1994;266(5191):1719-23.
26. Rodriguez-Viciana P, Warne PH, Dhand R, Vanhaesebroeck B, Gout I, Fry MJ, et al. Phosphatidylinositol-3-OH kinase as a direct target of Ras. Nature. 1994;370(6490):527-32.
27. McCubrey JA, Steelman LS, Chappell WH, Abrams SL, Wong EW, Chang F, et al. Roles of the Raf/MEK/ERK pathway in cell growth, malignant transformation and drug resistance. Biochim Biophys Acta. 2007;1773(8):1263-84. PMCID: 2696318.

28. Vizan P, Boros LG, Figueras A, Capella G, Mangues R, Bassilian S, et al. K-ras codon-specific mutations produce distinctive metabolic phenotypes in NIH3T3 mice [corrected] fibroblasts. Cancer Res. 2005;65(13):5512-5.
29. Ramanathan A, Wang C, Schreiber SL. Perturbational profiling of a cell-line model of tumorigenesis by using metabolic measurements. Proc Natl Acad Sci U S A. 2005;102(17):5992-7. PMCID: 1087961.
30. Telang S, Yalcin A, Clem AL, Bucala R, Lane AN, Eaton JW, et al. Ras transformation requires metabolic control by 6-phosphofructo-2-kinase. Oncogene. 2006;25(55):7225-34.
31. Moul JW, Friedrichs PA, Lance RS, Theune SM, Chang EH. Infrequent RAS oncogene mutations in human prostate cancer. Prostate. 1992;20(4):327-38.
32. Shimizu K, Goldfarb M, Suard Y, Perucho M, Li Y, Kamata T, et al. Three human transforming genes are related to the viral ras oncogenes. Proc Natl Acad Sci U S A. 1983;80(8):2112-6. PMCID: 393767.
33. McGrath JP, Capon DJ, Smith DH, Chen EY, Seeburg PH, Goeddel DV, et al. Structure and organization of the human Ki-ras proto-oncogene and a related processed pseudogene. Nature. 1983;304(5926):501-6.
34. Abubaker J, Bavi P, Al-Haqawi W, Sultana M, Al-Harbi S, Al-Sanea N, et al. Prognostic significance of alterations in KRAS isoforms KRAS-4A/4B and KRAS mutations in colorectal carcinoma. J Pathol. 2009;219(4):435-45.
35. Jancik S, Drabek J, Radzioch D, Hajduch M. Clinical relevance of KRAS in human cancers. J Biomed Biotechnol. 2010;2010:150960. PMCID: 2896632.
36. Dote H, Toyooka S, Tsukuda K, Yano M, Ouchida M, Doihara H, et al. Aberrant promoter methylation in human DAB2 interactive protein (hDAB2IP) gene in breast cancer. Clin Cancer Res. 2004;10(6):2082-9.
37. Min J, Zaslavsky A, Fedele G, McLaughlin SK, Reczek EE, De Raedt T, et al. An oncogene-tumor suppressor cascade drives metastatic prostate cancer by coordinately activating Ras and nuclear factor-kappaB. Nat Med. 2010;16(3):286-94. PMCID: 2903662.
38. Wang Z, Tseng CP, Pong RC, Chen H, McConnell JD, Navone N, et al. The mechanism of growth-inhibitory effect of DOC-2/DAB2 in prostate cancer. Characterization of a novel GTPase-activating protein associated with N-terminal domain of DOC-2/DAB2. J Biol Chem. 2002;277(15):12622-31.
39. Konstantinopoulos PA, Karamouzis MV, Papavassiliou AG. Post-translational modifications and regulation of the RAS superfamily of GTPases as anticancer targets. Nat Rev Drug Discov. 2007;6(7):541-55.
40. Willumsen BM, Christensen A, Hubbert NL, Papageorge AG, Lowy DR. The p21 ras C-terminus is required for transformation and membrane association. Nature. 1984;310(5978):583-6.
41. Manne V, Roberts D, Tobin A, O'Rourke E, De Virgilio M, Meyers C, et al. Identification and preliminary characterization of protein-cysteine farnesyltransferase. Proc Natl Acad Sci U S A. 1990;87(19):7541-5. PMCID: 54783.
42. Ali BR, Nouvel I, Leung KF, Hume AN, Seabra MC. A novel statin-mediated "prenylation block-and-release" assay provides insight into the membrane targeting mechanisms of small GTPases. Biochem Biophys Res Commun. 2010;397(1):34-41. PMCID: 2908739.
43. Demierre MF, Higgins PD, Gruber SB, Hawk E, Lippman SM. Statins and cancer prevention. Nat Rev Cancer. 2005;5(12):930-42.
44. Reiss Y, Goldstein JL, Seabra MC, Casey PJ, Brown MS. Inhibition of purified p21ras farnesyl:protein transferase by Cys-AAX tetrapeptides. Cell. 1990;62(1):81-8.
45. Lerner EC, Qian Y, Blaskovich MA, Fossum RD, Vogt A, Sun J, et al. Ras CAAX peptidomimetic FTI-277 selectively blocks oncogenic Ras signaling by inducing cytoplasmic accumulation of inactive Ras-Raf complexes. J Biol Chem. 1995;270(45):26802-6.
46. Chang TY, Chang CC, Ohgami N, Yamauchi Y. Cholesterol sensing, trafficking, and esterification. Annu Rev Cell Dev Biol. 2006;22:129-57.
47. Goldstein JL, Brown MS. Regulation of the mevalonate pathway. Nature. 1990;343(6257):425-30.
48. Song BL, Javitt NB, DeBose-Boyd RA. Insig-mediated degradation of HMG CoA reductase stimulated by lanosterol, an intermediate in the synthesis of cholesterol. Cell Metab. 2005;1(3):179-89.
49. Nguyen AD, McDonald JG, Bruick RK, DeBose-Boyd RA. Hypoxia stimulates degradation of 3-hydroxy-3-methylglutaryl-coenzyme A reductase through accumulation of lanosterol and hypoxia-inducible factor-mediated induction of insigs. J Biol Chem. 2007;282(37):27436-46.
50. Huggins C, Stevens RE, Jr. , Hodges CV. Studies on prostatic cancer: II. The effects of castration on advanced carcinoma of the prostate gland. Arch Surg. 1941;43(2):209-23.
51. Feldman BJ, Feldman D. The development of androgen-independent prostate cancer. Nat Rev Cancer. 2001;1(1):34-45.
52. Yu M, Zhou Y, Shi Y, Ning L, Yang Y, Wei X, et al. Reduced mitochondrial DNA copy number is correlated with tumor progression and prognosis in Chinese breast cancer patients. IUBMB Life. 2007;59(7):450-7.
53. Tseng LM, Yin PH, Chi CW, Hsu CY, Wu CW, Lee LM, et al. Mitochondrial DNA mutations and mitochondrial DNA depletion in breast cancer. Genes Chromosomes Cancer. 2006;45(7):629-38.
54. Hobisch A, Culig Z, Radmayr C, Bartsch G, Klocker H, Hittmair A. Distant metastases from prostatic carcinoma express androgen receptor protein. Cancer Res. 1995;55(14):3068-72.

55. Chin MH, Qian WJ, Wang H, Petyuk VA, Bloom JS, Sforza DM, et al. Mitochondrial dysfunction, oxidative stress, and apoptosis revealed by proteomic and transcriptomic analyses of the striata in two mouse models of Parkinson's disease. J Proteome Res. 2008;7(2):666-77.
56. Moro L, Arbini AA, Yao JL, di Sant'Agnese PA, Marra E, Greco M. Mitochondrial DNA depletion in prostate epithelial cells promotes anoikis resistance and invasion through activation of PI3K/Akt2. Cell Death Differ. 2009;16(4):571-83.
57. Tsuruzoe K, Araki E, Furukawa N, Shirotani T, Matsumoto K, Kaneko K, et al. Creation and characterization of a mitochondrial DNA-depleted pancreatic beta-cell line: impaired insulin secretion induced by glucose, leucine, and sulfonylureas. Diabetes. 1998;47(4):621-31.
58. Moraes CT, Shanske S, Tritschler HJ, Aprille JR, Andreetta F, Bonilla E, et al. mtDNA depletion with variable tissue expression: a novel genetic abnormality in mitochondrial diseases. Am J Hum Genet. 1991;48(3):492-501. PMCID: 1682992.
59. Spelbrink JN, Van Galen MJ, Zwart R, Bakker HD, Rovio A, Jacobs HT, et al. Familial mitochondrial DNA depletion in liver: haplotype analysis of candidate genes. Hum Genet. 1998;102(3):327-31.
60. Rotig A, Poulton J. Genetic causes of mitochondrial DNA depletion in humans. Biochim Biophys Acta. 2009;1792(12):1103-8.

Appendix:

Fig. 1: The copy number of the mitochondrial genome content in a single cell from a human PCa specimen is amplified, and, subsequentially, depleted with the clinical progression of the disease. Graphed is a QRT-PCR of the (mitochondrial-encoded) ND1 gene in the total-DNA lysates from single cells collected from human PCa specimens. Single cells were isolated with laser microdissection from human PCa tumors of a high or low Gleason grade (6-7 or 8-9, respectively), in addition to, prostate epithelial cells from adjunct-normal tissue. A student's t-test was conducted to compare the copy number of the mitochondrial genome content in PCa cells from tumors of a low Gleason grade, with respect to normal prostate epithelial cells *($p < 0.01$) or tumors of a high Gleason grade **($p < 0.01$). The sample number of the single cells from low grade, high grade, and normal specimens was n = 8, 8, and 6 respectively.

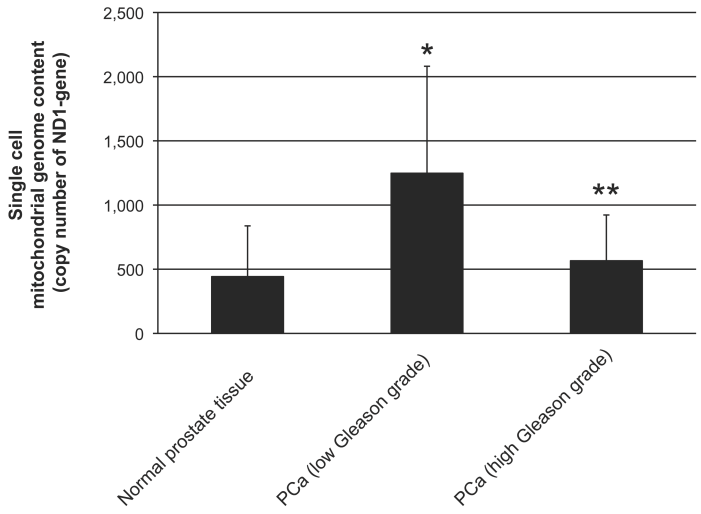

Fig. 2: The copy number of the mitochondrial genome content within single cells of PCa is inversely associated with the CR phenotype. Graphed is a QRT-PCR of the (mitochondrial-encoded) ND1 gene in total-DNA lysate from single cells collected from normal prostate epithelial cells (PrEC), early stage PCa (LNCaP), and CR PCa (C4-2, PC-3, and DU-145). It is important to note that C4-2 was derived from the *in vivo* progression of LNCaP to a CR phenotype. The sample number of single cells for each cell line was ten (n = 10).

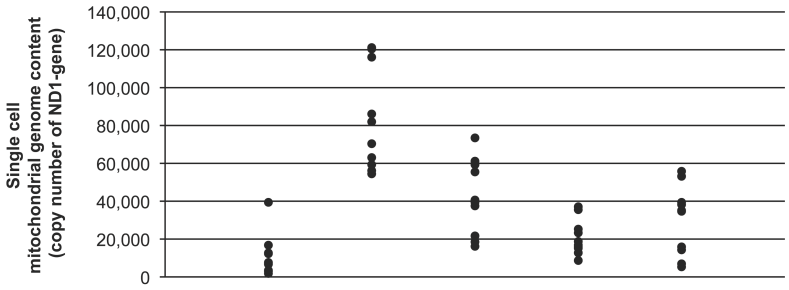

	PrEC	LNCaP	C4-2	PC-3	DU-145
Average	11,054	82,904	42,323	20,918	29,872
SD	5,055	25,963	19,699	9,933	19,089
Median	7,272	76,172	40,014	17,788	34,875
Minimum	1,828	54,455	16,160	8,670	5,320
Maximum	39,403	121,157	73,433	37,069	55,801

Fig. 3: GTP-bound (activated) Ras-GTPase are progressively generated with the reduction-to-depletion of the mitochondrial genome content in PCa. Depicted is a western blot of GTP-bound Ras pulled-down from 160 μg of total-protein lysates collected from normal prostate epithelial cells (PrEC), early-stage PCa (LNCaP), and CR PCa (C4-2, PC-3, DU-145 and LNρ0-8). It is important to note that C4-2 and LNρ0-8 were derived from the progression of LNCaP to an advanced disease, *in vitro and in vivo*, respectively. A Ras Activation Assay Kit was used to pulled-down GTP-bound Ras from lysates, utilizing agarose beads conjugated to the RBD of raf-1 as recommended by the manufactures protocol. Pull-downs of lysates were subjected to 18% SDS-PAGE, and subsequentially transferred onto membrane to be probed with anti-total Ras.

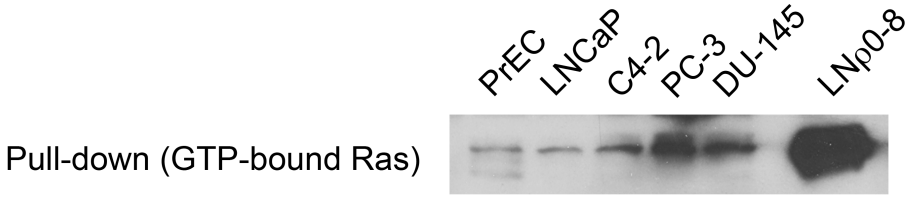

Fig. 4. The copy number of the mitochondrial genome in PCa is inversely associated with the 'oxic state' of the disease. Depicted is an O_2 concentration assay of normal prostate epithelial cells (PrEC), early-stage PCa (LNCaP), and CR PCa (C4-2, PC-3, DU-145, and LNρ0-8). It is important to note that C4-2 and LNρ0-8 were derived from the progression of LNCaP to an advanced disease, *in vitro and in vivo*, respectively. The denoted cell lines were transferred into a 96 well OxoPlate at the denoted concentrations. The O_2 concentration in the cell culture media was quantified with oxygen-sensors in the OxoPlate and a spectrophotometer for 2 hours of incubation. The data was reported as the mean ± SE (n = 3).

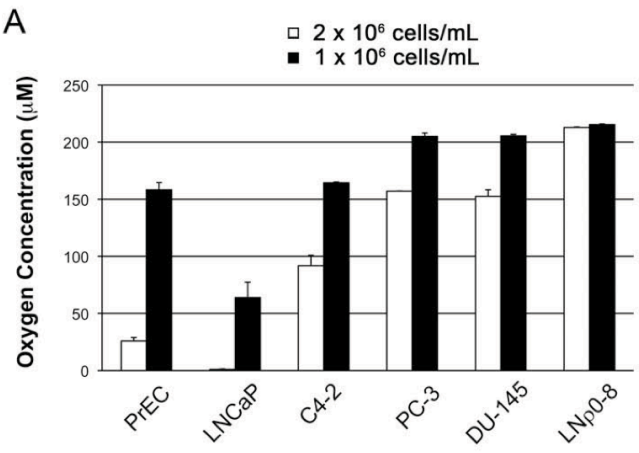

Fig. 5: The cellular expression of AR is diminished in response to the constitutive activation of ERK that develops from the depletion of the mitochondrial genome in PCa. Depicted is a western blot of AR in 60 μg of total-protein lysates collected from ρ0 of LNCaP (LNρ0-8) that was cultured 48 hr in the absence or presence of PD98059 to inhibit the phosphorylation of ERK. Total-protein lysates were subjected to 8% SDS-PAGE, and subsequentially transferred onto membrane to be probed with anti-AR, anti-total-ERK, anti-phospho ERK to confirm the phosphorylation status of ERK, and anti-β-actin as a loading control. LNCaP were evaluated as a positive control for the AR and as a negative control for phospho-ERK.

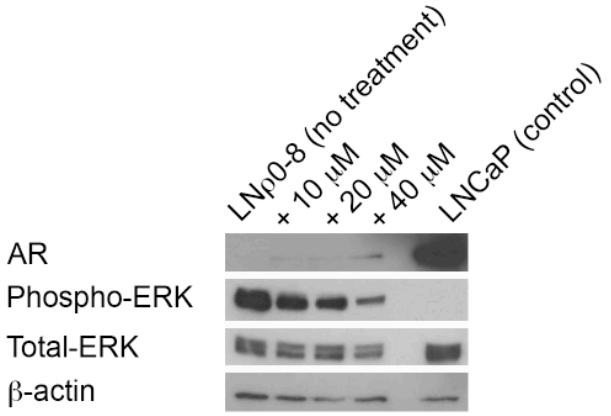

Fig. 6: The cellular expression of AR is diminished in response to the constitutive activation of ERK that follows the depletion of the mitochondrial genome content from PCa (LNCaP). Depicted is a western blot of AR in 60 μg of total-protein lysates collected from ρ0 of LNCaP (LNρ0-8) that was cultured 48 hr in the absence or presence of, either, GW5074 or U0126 to inhibit the phosphorylation of ERK. Total-protein lysates were subjected to 8% SDS-PAGE, and subsequentially transferred to membrane to be probed with anti-AR, anti-total-ERK, anti-phospho ERK to confirm the phosphorylation status of ERK, and anti-β-actin as a loading control. LNCaP were evaluated as a positive control for the AR and as a negative control for phospho-ERK.

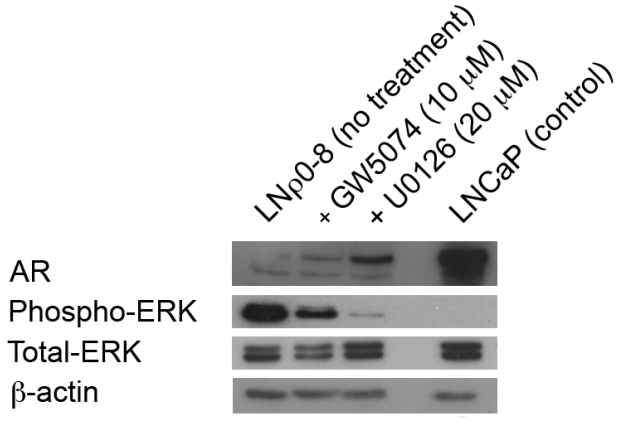

Fig. 7: The cellular transcription of AR is diminished in response to the constitutive activation of ERK that follows the depletion of the mitochondrial genome content from PCa (LNCaP). Depicted is the RT-PCR of the AR transcripts in 200 ng of total-cDNA constructed from total-RNA lysates collected from ρ0 of LNCaP (LNρ0-8) cultured 48 hr in the absence or presence of U0126, or PD98059, GW5074 to inhibit the phosphorylation of ERK. LNCaP was evaluated as a positive control for AR. It is important to note that the results are preliminary, due to the absence of re-expression of AR at high dose of PD98059 and GW5074. Repetition should include a proper loading control, such as GAPDH.

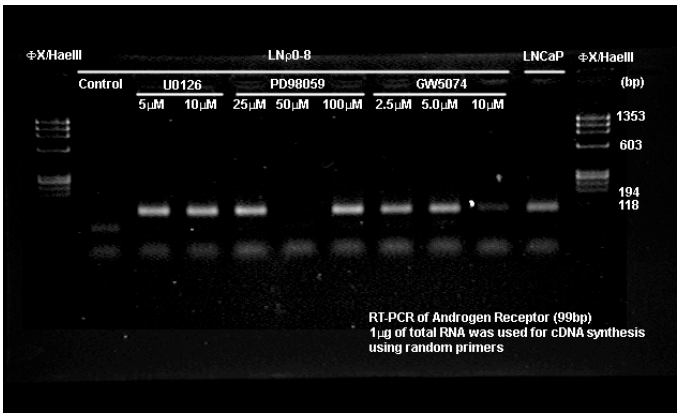

Fig. 8: LNCaP is sensitive to anti-androgen, flutamide. Depicted is a graph of the viability of LNCaP that was seeded at a concentration of 2,000 cells/well in a 96 well plate, overnight. Cells were cultured 4 days in the absence (control) or presence of flutamide at the denoted dosages (n = 3). After treatment, the viability of cells was quantified in a calcein assay and the mean of each group was reported as a relative percent to the control (arbitrary unit ± SE). A student's t-test was conducted to compare samples to the control (*$p < 0.05$ and **$p < 0.001$). Error bars represent standard error.

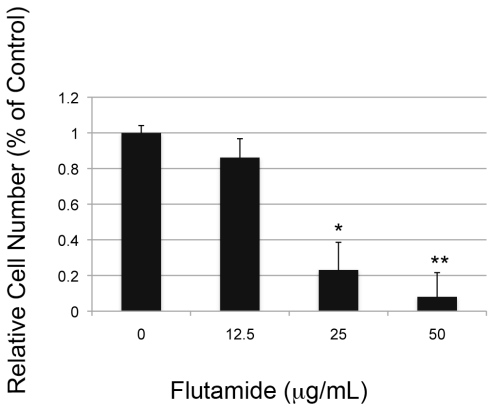

Fig. 9: A flux in the mevalonate-to-Ras pathway, generated from the depletion of the mitochondrial genome content, in PCa advances the disease to the AAR phenotype. Depicted is a graph of the viability of LNρ0-8 that was seeded at a concentration of 2,000 cells/well in a 96 well plate, overnight. Cells were cultured 4 days in the absence or presence of flutamide at the denoted dosage. Cells cultures were additionally supplemented without (control) or with 40 μM PD98059 (n = 3). After treatment, the viability of cells was quantified in a calcein assay and the mean of each group was reported as a relative percent to the control, 0 μg/mL Flutamide (arbitrary unit ± SE). A student's t-test was conducted to compare the viability of cells exposed to control and PD98059 conditions in the same dosage of flutamide (*$p < 0.001$). Error bars represent standard error.

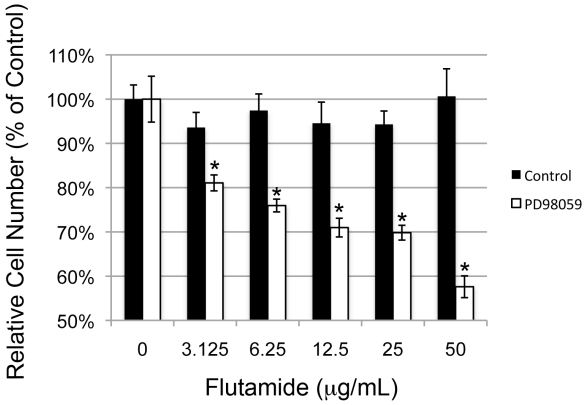

Citation: Cell Death and Disease (2012) 3, e258; doi:10.1038/cddis.2011.141

www.nature.com/cddis

Consumption of oxygen: a mitochondrial-generated progression signal of advanced cancer

CC Cook[1], A Kim[1], S Terao[2,3], A Gotoh[2,3] and M Higuchi*[,1]

Changes in mitochondrial genome such as mutation, deletion and depletion are common in cancer and can determine advanced phenotype of cancer; however, detailed mechanisms have not been elucidated. We observed that loss of mitochondrial genome reversibly induced overexpression and activation of proto-oncogenic Ras, especially K-Ras 4A, responsible for the activation of AKT and ERK leading to advanced phenotype of prostate and breast cancer. Ras activation was induced by the overexpression of 3-hydroxy-3-methyl-glutaryl-CoA reductase (HMGR), the rate-limiting enzyme of the mevalonate pathway. Hypoxia is known to induce proteasomal degradation of HMGR. Well differentiated prostate and breast cancer cells with high mitochondrial DNA content consumed a large amount of oxygen and induced hypoxia. Loss of mitochondrial genome reduced oxygen consumption and increased in oxygen concentration in the cells. The hypoxic-to-normoxic shift led to the overexpression of HMGR through inhibiting proteasomal degradation. Therefore, reduction of mitochondrial genome content induced overexpression of HMGR through hypoxic to normoxic shift and subsequently the endogenous induction of the mevalonate pathway activated Ras that mediates advanced phenotype. Reduction of mitochondrial genome content was associated with the aggressive phenotype of prostate cancer *in vitro* cell line model and tissue specimens *in vivo*. Our results elucidate a coherent mechanism that directly links the mitochondrial genome with the advanced progression of the disease.
Cell Death and Disease (2012) **3,** e258; doi:10.1038/cddis.2011.141; published online 19 January 2012
Subject Category: Cancer

Prostate cancer (PCa) is a significant health problem, representing the leading cancer diagnosis and the second leading cause of cancer death in North American men.[1] PCa begins as an androgen-dependent cancer that undergoes clinical regression in response to pharmacological or surgical strategies that reduce testosterone concentration. Despite this treatment, the cancer frequently recurs as an androgen-independent or castration-resistant cancer with metastatic phenotype. Therefore, elucidation of the mechanisms involved in the development to an aggressive metastatic phenotype is a critical topic.

Mitochondria are essential organelles that generate ATP through oxidative phosphorylation. This process is accomplished by a series of protein complexes and mitochondrial respiratory chains encoded by nuclear DNA (nDNA) and mitochondrial DNA (mtDNA). Human mtDNA is remarkably small (16 569 bp) compared with nDNA ($\sim 10^9$ bp) and encodes 13 proteins in the mitochondrial respiratory chains (MRC), 22 transfer RNAs, and 2 ribosomal RNAs.[2]

Several reports showed that mutations of mtDNA had been identified in various types of cancer, including breast, colon, prostate, pancreatic and other cancers.[3] The growth advantage of cancer cells with specific mutant mtDNA has also been demonstrated in an *in vivo* mouse model system using cybrid (trans-mitochondrial hybrid) cells, suggesting that specific mutations of mtDNA give a survival advantage and induce metastasis.[4] In PCa specimens, Chen *et al*.[5] reported an extremely high incidence of somatic mutation (90%) in the D-loop region that may cause reduction of mtDNA content.[6]

The roles of mtDNA and mitochondrial respiratory function in biological functions has been demonstrated using mtDNA-deficient cells.[7] We previously showed that TNF and serum starvation could not induce apoptosis in mtDNA-depleted cells, whereas they induced apoptosis in parental cells and cells reconstituted with normal mtDNA.[8] These results indicate that mitochondrial respiratory function and mtDNA are critically important in apoptosis. We showed following observations to demonstrate the mechanisms involved in the induction of advanced phenotype of PCa by the reduction of mitochondrial genome content. Reduction of mtDNA content shifted (1) androgen-dependent PCa cells to an androgen-independent phenotype *in vitro* and *in vivo*[9] and induced (2) epithelial-to-mesenchymal transition changes that may lead to PCa progression,[10] (3) hypermethylation of CpG islands of the putative tumor suppressor genes[11] and (4) abnormal activation of NF-κB,[12] AP-1,[12] AKT,[13] ERK[10] and JNK[10] that may lead to aggressive phenotype in PCa progression.

[1]Department of Biochemistry and Molecular Biology, University of Arkansas for Medical Sciences, Little Rock, AR, USA; [2]Laboratory of Cell and Gene Therapy, Institute for Advanced Medical Sciences, Hyogo College of Medicine, Nishinomiya, Japan and [3]Advanced Medicinal Research Center, Hyogo University of Health Science, Kobe, Japan
*Corresponding author: M Higuchi, Department of Biochemistry and Molecular Biology, University of Arkansas for Medical Sciences, Little Rock, AR 72205, USA. Tel: +1 501 526 7520; Fax: +1 501 686 8169; E-mail: mhiguchi@uams.edu
Keywords: 3-hydroxy-3-methyl-glutaryl-CoA reductase; hypoxia; mitochondrial DNA; prostate cancer; Ras
Abbreviations: HMGR, 3-hydroxy-3-methyl-glutaryl-CoA reductase; nDNA, nuclear DNA; mtDNA, mitochondrial DNA; PCa, prostate cancer; MRC, mitochondrial respiratory chains; FISH, fluorescent *in situ* hybridization; DAB2IP, DOC-2/DAB2 interactive protein; PrEC, prostate epithelial cells; FPP, Farnesyl pyrophosphate; FTase, farnesyltransferase; FTI, farnesyltransferase inhibitor; ALLN, N-[N-(N-Acetyl-L-leucyl)-L-leucyl]-L-norleucine; mitoGPS, mitochondrial-generated progression signal
Received 30.9.11; revised 15.11.11; accepted 21.11.11; Edited by A Finazzi-Agró

Ras-GTPases are potential candidates that can transduce the constitutive and concurrent activation of a broad array of effectors such as ERK and AKT. As small GTPases, Ras are dynamically activated and inactivated with the association of GTP or GDP, respectively. Human cancers (~25%) often harbor (oncogenic) mutations in Ras that disable the ability of the GTPases to dynamically be inactivated, leading to the constitutive and concurrent activation of a diverse array of signal pathways, for example, Raf/MEK/ERK and PI3K/Akt.[14] Although tissue studies have revealed the constitutive and concurrent activation of ERK and Akt in the progression of PCa, the majority of PCa tumors do not harbor RAS mutation (oncogenes).[15] Yet, it is generally acknowledged that the aberrant activation of Ras can shift PCa from androgen-dependent to independent,[16] whereas the expression of dominant-negative Ras attenuates androgen-independent phenotype,[17] indicating that Ras activation is responsible for the phenotype of PCa. In the current study of PCa, we investigated a pathway of metabolic and proto-oncogenic processes including Ras activation that aberrantly activates ERK and Akt. We denoted this as the mitochondrial-generated progression signal (mitoGPS) that transduces changes in mitochondrial genome in the early-stages of PCa into the advanced progression of the disease.

Results

Reduction of the mitochondrial genome content is associated with PCa progression. We first investigated whether mitochondrial genome content changes associated with aggressive phenotype of PCa in human tissue specimens. Mitochondrial genomic analysis in a single cell revealed that the mitochondrial genome copy-number/cell was significantly reduced in high-grade tumors (Gleason grade 8 and 9) as compared with that in low-grade tumors (Gleason grade 6 and 7) (Figure 1a) ($P<0.01$). The *in vivo* observations were verified in human cell lines the early stages androgen-dependent PCa (LNCaP), or an array of PCa (C4-2, PC-3 and DU-145). Classical cell lines for the *in vitro* evaluation of PCa, include: the castration sensitive LNCaP established from a metastatic (supraclavicular lymph node) lesion of human prostate adenocarcinoma;[18] the castration resistant (CR) C4-2 isolated from recurrent tumors that develop after castration of mice inoculated with LNCaP;[19] and CR PCa cell lines derived from metastasis in human bone (PC-3) and brain (DU-145).[20,21] In the current study, mitochondrial genomic analysis showed a low mitochondrial genome content in PC-3 and DU-145, in addition to a significant reduction in C4-2, relative to the parental LNCaP (Figure 1b).

Reduction of the mitochondrial genome content reversibly induces the aberrant activation of ERK and Akt. We evaluated the biological impact of the reduction of the mitochondrial genome content in the progression of PCa by the experimental depletion of the genome from LNCaP. We additionally utilized the MCF-7 cell line, a classical breast cancer (BCa) established from the metastasis (pleural effusion) of a human breast adenocarcinoma.[22] The knock-out of the mtDNA (mtDNA-KO) from LNCaP and MCF-7 was demonstrated in the creation of the LNρ0-8 and MCFρ0 cell lines, respectively.[9,10] To confirm that experimental observations that follow the loss of the mitochondrial genome content are not of consequence to an incidental mutation to the nuclear genome induced by ethidium bromide treatment, the mitochondrial genome was reconstituted to the mtDNA-KO cell lines (LNρ0-8 and MCFρ0) in the creation of the mtDNA-knock in (mtDNA-KI) cells lines, denoted as LNCyb and MCFCyb.

The mitochondrial genome contents of the indicated cell lines were visually confirmed by fluorescent *in situ* hybridization (FISH). Mitochondria were labeled with MitoTracker Red and showed that presence of mitochondria in parental, mtDNA-KO and mtDNA-KI cells (Figure 1c). Microscopic (confocal) images also show the abundance of the mtDNA probes localized in the mitochondria of the parental and mtDNA-KI cells; no mtDNA probes were observed in the mtDNA-KO cells (Figure 1c). The results were confirmed by the quantification of the mitochondrial genome content by QRT-PCR (Figure 1d); the mitochondrial genome content in LNCyb and MCFCyb was partially or completely restored, respectively, to that in LNCaP and MCF-7. We observed that the amount of ATP in LNCaP was significantly reduced in LNr0-8 (113.3 ± 2.0 and 73.2 ± 2.1 nM/mg protein, respectively) (average $\pm$ S.E., P-value $= 0.0056$) and lactate generation was increased (1463 ± 66 and 3416 ± 82 nM, respectively) (average $\pm$ S.E., P-value $= 0.000049$). The results suggest that loss of mitochondrial genome reduced ATP generation possibly by the reduction of oxidative phosphorylation that might increase in anaerobic glycolysis.

It is well documented that ERK and Akt are constitutively activated in the progression of advanced PCa tumors.[15] Our data reveal ERK and Akt to be constitutively activated in the mtDNA-KO of PCa and BCa, relative to the parental and mtDNA-KI cells (Figure 1e). Of the ERKs, that is, ERK1 (p44) and ERK2 (p42), ERK2 was the most dramatically phosphorylated in LNρ0-8 and MCFρ0.

Reduction of the mitochondrial genome content in PCa and BCa constitutively activates Ras. The interaction of activated GTP-bound Ras with the Ras binding domain (RBD) of Raf-1,[23] generates GTP-bound Ras–Raf complexes that lead to the activation of ERK and Akt.[24,25] We investigated whether Ras is activated by depletion of mitochondrial genome. No active Ras was pulled-down from the total-protein lysates (160 μg) of parental (LNCaP and MCF-7) cells in comparison with a positive control (Figure 2a). Meanwhile, active Ras from mtDNA-KO was observed even when the quantity of LNρ0-8 and MCFρ0 lysates probed was reduced to 0.5 μg or 5 μg, respectively, active Ras was observed as two bands of intensity similar to the positive control (Figure 2a). The experiment demonstrates that the depletion of the mitochondrial genome in PCa leads to the constitutive activation of Ras. Association of the reduction of mitochondrial genome content with the activation of Ras was verified in an array of PCa C4-2, PC-3 and DU-145 that harbor low mitochondrial

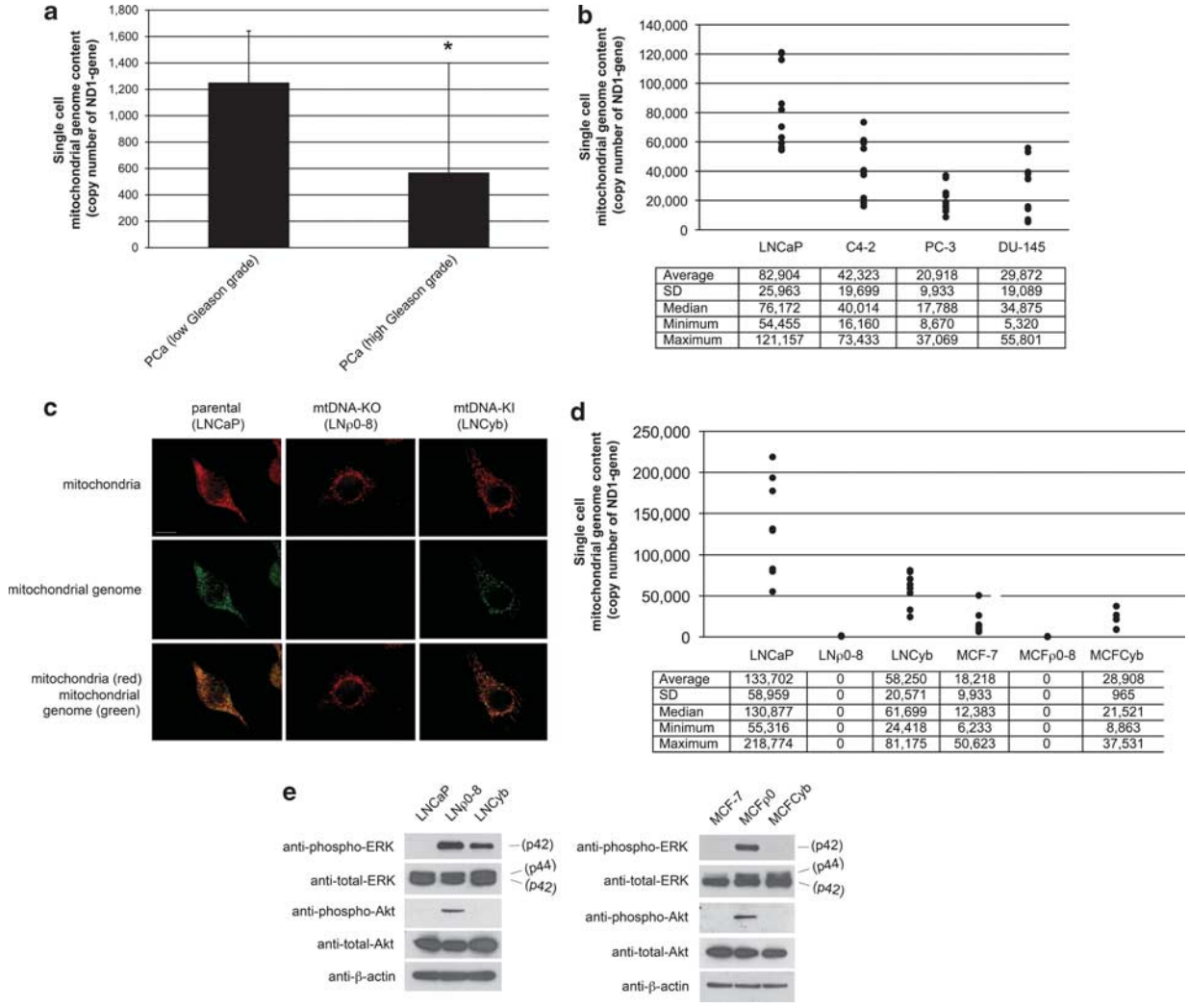

Figure 1 Reduction of the mitochondrial genome content in PCa and BCa reversibly induced aberrant activation of ERK and AKT. (**a**) Mitochondrial genome content per cell in low (6–7) and high (8–9) Gleason grade PCa separated by laser microdissection. Student's *t*-test compared PCa with a high Gleason grade (*$P<0.01$) ($n=8$ and 6, respectively). (**b**) Mitochondrial genome contents of single cells ($n=10$) of an early-stage (LNCaP) PCa cell line, and an array of (C4-2, PC-3 and DU-145) PCa cell lines. (**c**) FISH of the mitochondrial genome. Green: mitochondrial genome. Red: mitochondria. Scale bar represents 20 μm. (**d**) Mitochondrial genome content in single cells ($n=8$) of the parental (LNCaP and MCF-7), mtDNA-KO (LNρ0-8 and MCFρ0) and mtDNA-KI (LNCyb and MCFCyb) cells. (**e**) Phospho-ERK, total ERK, phospho-Akt, total AKT and β-actin in total-protein lysates (30 μg) of the indicated cell lines

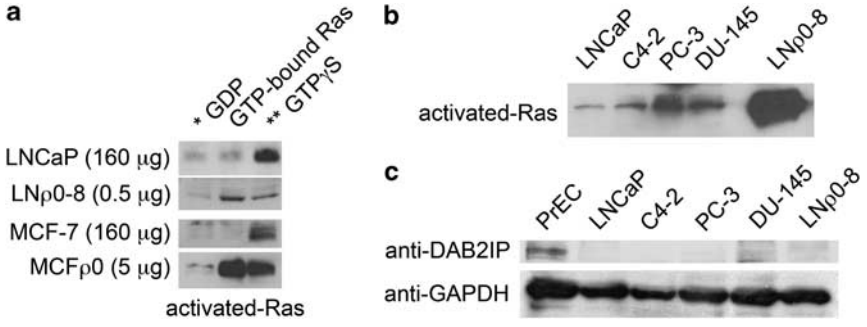

Figure 2 Reduction of the mitochondrial genome content in PCa and BCa constitutively activates Ras. (**a**) Activated (GTP-bound) Ras was pulled down and determined by western blotting. Negative controls (*GDP) and positive controls (**GTPγS): before pull-down, an aliquot of total protein lysate was pre-loaded with GDP or GTPγS, respectively. (**b**) Activated Ras in total-protein lysates (160 μg) of the indicated PCa cells lines. (**c**) DAB2IP in total-protein lysates (90 μg) of normal PrEC and the indicated PCa cell lines

genome contents, relative to the early stages of PCa LNCaP (Figures 1b and 2b).

The shift of normal epithelial cells to the early-stages of PCa and BCa is associated with the genetic silencing of RasGAPs, particularly the DOC-2/DAB2 interactive protein (DAB2IP).[26] The attenuation of DAB2IP activity in PCa diminishes the cells ability to amplify the GTPase activity of Ras, leading to the prolonged accumulation of active GTP-bound Ras.[27] We observed the expression of DAB2IP to be expressed in the prostate epithelial cells (PrEC), but not in all PCa including LNCaP, C4-2, DU-145 and PC-3 (Figure 2c). Collectively the experiments demonstrate that the shift of normal prostate epithelial cells to PCa is associated with a silencing of a RasGAP that is not enough to explain why Ras is not activated in early stages of PCa LNCaP.

Reduction of the mitochondrial genome content in PCa overexpresses proto-oncogenic K-Ras 4A. The human cell contains three nuclear-encoded RAS genes that encode four isoforms of Ras: H-Ras, N-Ras and two splice variations of K-Ras, K-Ras 4A and K-Ras 4B. We observed the protein level of K-Ras 4A to be greatly elevated in the mtDNA-KO (LNρ0-8 and MCFρ0), relative to the parental cells. Reconstitution of the mitochondrial genome to the mtDNA-KO attenuated the aberrant K-Ras 4A expression (Figure 3a). Expression level of K-Ras 4A in mtDNA-KO cells was exceptionally high as compared with that of K-Ras 4B, H-Ras and N-Ras. A similar expression pattern was observed for the transcript levels of K-Ras 4A (Figure 3b). Association of the reduction of mitochondrial genome content with increased expression of K-Ras 4A was verified in an array of PCa C4-2, PC-3 and DU-145 that harbor low mitochondrial genome contents, relative to the early stages of PCa LNCaP (Figures 1b and 3c).

We note that the constitutive activation of Ras observed with the depletion of the mitochondrial genome was not a consequence of oncogenic mutation in nucleotide sequences that encode for codons 12, 13 or 61 of K-Ras.[28] In a subsequent experiment we demonstrated that silencing of K-RAS in LNρ0-8, by transfection of K-RAS siRNA, reduced the expression of K-Ras 4A and the phosphorylation of ERK and Akt, but not total ERK nor total AKT (Figure 3d). Collectively, the experiments demonstrate that the reduction of the mitochondrial genome leads to the aberrant expression and activation of Ras, predominantly proto-oncogenic K-Ras 4A, and a process that is reversible with the reconstitution of the mitochondrial genome.

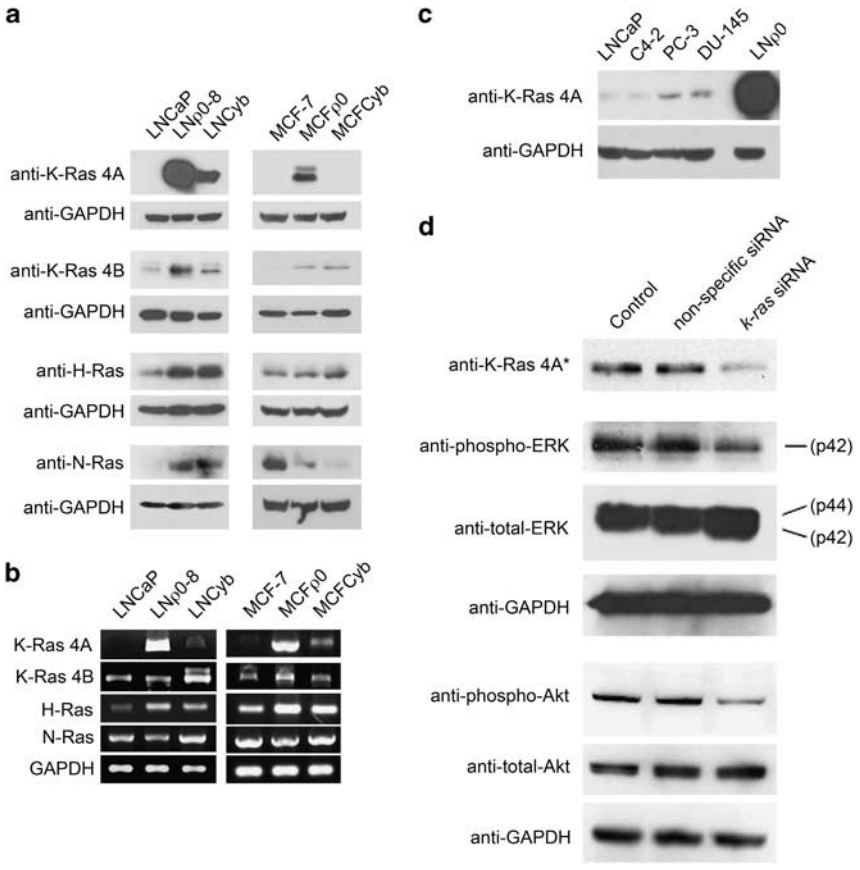

Figure 3 Reduction of the mitochondrial genome content in PCa overexpresses proto-oncogenic K-Ras 4A. (**a**) Ras isoforms in total protein lysates (30 μg) of the indicated cell lines. Exposure time was 10 s, excluding K-Ras 4A (0.5 s). (**b**) RT-PCR analysis of Ras (cDNA) transcripts in total-cDNA constructed from total-RNA lysates of the indicated cell lines. (**c**) K-Ras 4A in total-protein lysates (30 μg) of the indicated cell lines. (**d**) Phospho-ERK and phospho-Akt in total-protein lysates (30 μg) of LNρ0-8 transfected in the absence (control) or presence of K-RAS siRNA or non-specific siRNA. Protein levels of K-Ras 4A were evaluated in *(0.5 μg) total-protein lysates

HMGR (3-hydroxy-3-methyl-glutaryl-CoA reductase) expression is responsible for the aberrant activation of Ras mediated by the reduction of the mitochondrial genome content. Ras must translocate to cellular membrane by post-translational modifications that enable the (GTP-bound) Ras–Raf complexes to activate effectors at cellular membranes.[29] Localization of Ras to the cellular membrane is mediated by the prenylation of Ras, that is, the addition of farnesyl to the first cysteine (CAAX) of the C-terminus.[30] Farnesyl moieties for the prenylation of Ras are derived from farnesyl pyrophosphate, an intermediate of the mevalonate pathway that is catalytically transferred by farnesyltransferase (FTase).[31]

Immunohistochemical analysis confirmed that expression of Ras was greatly increased in LNρ0-8 as compared with LNCaP (Figure 4a). Figures 4a and b also demonstrates that Ras located only in cytosolic fraction in LNCaP and cellular membrane and certain organelle in LNρ0-8 suggesting that the depletion of the mitochondrial genome signals the localization of Ras to the cellular membrane and specific organelle. Farnesylation of Ras can be repressed with lovastatin-mediated inhibition of the rate-limiting step of the mevalonate pathway – the metabolism of HMG-CoA to mevalonate by HMGR.[32] Addition of lovastatin to the culture of LNρ0-8 generated the cytosolic accumulation of Ras, in addition to a shift to LNCaP-like cell morphology, both of which were reversed with co-application of exogenous mevalonate (Figure 4b). To directly inhibit the farnesylation of Ras, farnesyltransferase inhibitors (FTIs) have been designed as peptidomimetics of the C-terminus (CAAX) of Ras.[32] The supplementation of lovastatin or FTI-276 diminished the phosphorylation of ERK and Akt in LNρ0-8 (Figures 4c and d). The results suggest that the endogenous activity of the mevalonate pathway is necessary for the constitutive activation of Ras in LNρ0-8.

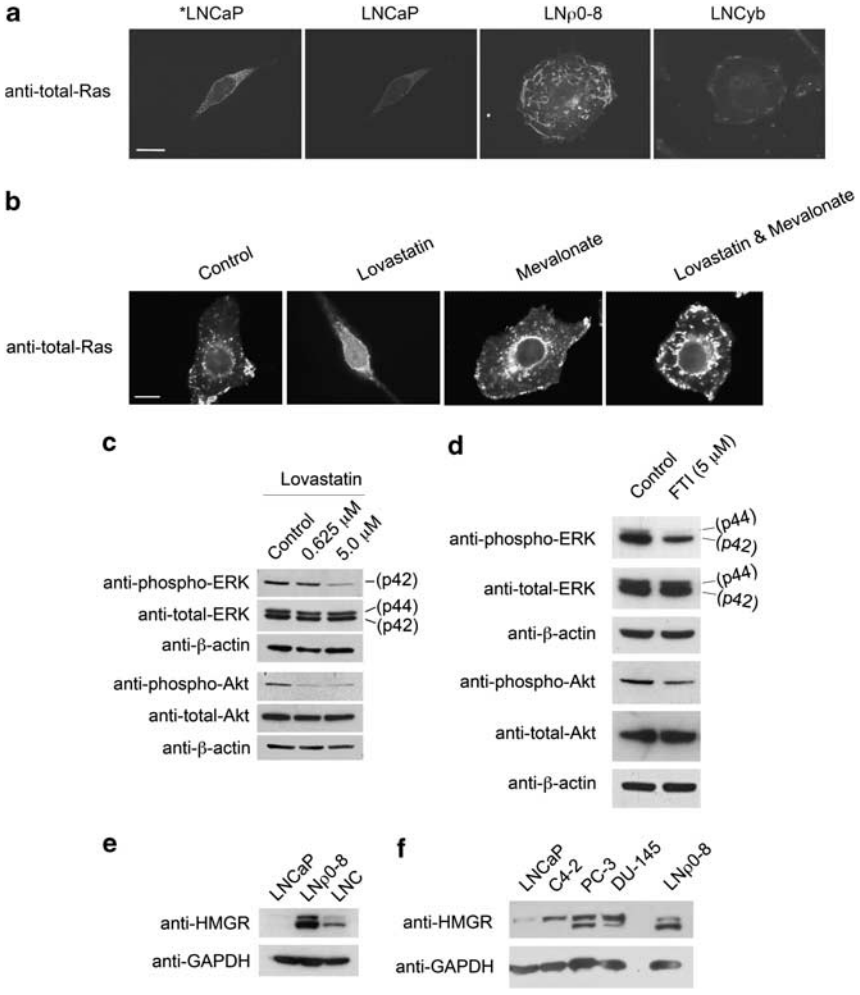

Figure 4 The endogenous mevalonate pathway mediates the maturation of aberrant Ras signals in PCa devoid of the mitochondrial genome. (**a**) Confocal images (z-slices) of anti-total-Ras (Alexa-488 labeled-anti-mouse IgG) within an intracellular plane of formaldehyde fixed cultures of the indicated cell lines. Matched image sets were mapped to a common linear gray-scale range (*overexposed image of LNCaP). Scale bars represent 20 μm. (**b**) Confocal images (z-slices) of anti-total-Ras in mtDNA-KO (LNρ0-8) cells cultured 12 h in the absence (control) or presence of lovastatin (5 μM) with or without mevalonate (1 mM). (**c** and **d**) Phospho-ERK, total ERK, phospho-Akt, total AKT and β-actin in total-protein lysates (30 μg) of LNρ0-8 cells cultured 24 h in the absence (control) or presence of lovastatin (**c**), or (**d**) 48 h in the absence (control) or presence of FTI-276. (**e**) HMGR in total-protein lysates (30 μg) of the parental, mtDNA-KO and mtDNA-KI of LNCaP. (**f**) HMGR in total-protein lysates (30 μg) of indicated cells as assessed by western blot with anti-HMGR

Then, we further investigated the potential cause for upregulation of mevalonate pathway. We observed an elevation of the expression of HMGR with the depletion of the mitochondrial genome (LNρ0-8) could be attenuated with the reconstitution of the genome (LNCyb) (Figure 4e). We also observed the expression of HMGR was enhanced associated with the reduction of the mitochondrial genome content in PCa cell lines (Figure 4f). These results indicate that an elevation in the endogenous expression of HMGR is responsible for the activation of Ras when the mitochondrial genome content is reduced.

Inhibition of mitochondrial respiration is responsible for HMGR *expression* possibly through the inhibition of proteasomal degradation. Mitochondrial genome encodes 13 proteins in MRC and therefore reduction of mitochondrial genome leads to the inhibition of mitochondrial respiration. To determine if the induction of HMGR expression is induced by the inhibition of mitochondrial respiration, LNCaP cells were cultured in the absence or presence of inhibitors of various complexes of the MRC: rotenone inhibits complex I; antimycin A inhibits complex III; oligomycin inhibits Fo-ATPase of complex V. Rotenone, antimycin A and oligomycin at the concentration used inhibited the oxygen consumption rate of LNCaP (32.6%, 35.2% and 34.4%, respectively) and enhanced the expression of HMGR (Figure 5a).

HMGR is regulated by multiple feedback mechanisms, including: transcriptional and/or translational regulation, PTMs, and/or proteasomal degradation by both sterol and non-sterol products of the mevalonate pathway.[33] We investigated whether proteasomal degradation is associated with high expression of HMGR. Incubation with proteasomal inhibitor N-[N-(N-Acetyl-L-leucyl)-L-leucyl]-L-norleucine (ALLN) in LNCaP increased the protein level of HMGR (Figure 5b), suggesting that early stage PCa maintain low expression level of HMGR by proteasomal degradation.

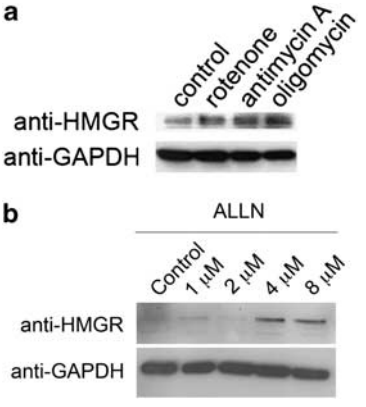

Figure 5 Inhibitors of mitochondrial respiratory chain and proteasomal degradation enhanced expression of HMGR. (**a**) HMGR expression and ERK phosphorylation were evaluated in total-protein-lysates (30 μg) of LNCaP cultured 6 h in the presence or absence of rotenone (400 nM), antimycin A (160 ng/ml) and oligomycin (8 μg/ml). (**b**) HMGR in total-protein lysates of LNCaP cultured 6 h in the absence (control) or presence of ALLN at the indicated dosages

HMGR expression in PCa is enhanced by the hypoxic-to-normoxic shift. A recent study has demonstrated that hypoxia induces the proteasomal degradation of HMGR.[34,35] As expected, oxygen consumption is well associated with the content of mitochondrial genome in PCa cell lines (Figures 1b and 6a). From this observation, we hypothesized that LNCaP cells induce hypoxia by high consumption rate of oxygen leading to hypoxia-induced HMGR degradation, and that in advanced PCa the hypoxic state is retarded with the inhibition of respiration, that is, by the reduction of mitochondrial genome content, leading to the accumulation of HMGR expression. Interestingly, the oxygen concentration of surrounding cells was greatly reduced with the culture of LNCaP and MCF-7, as observed with the induction of hypoxia (12.3 and 4.2 μM, respectively) in an hour (Figures 6b and c, respectively). The hypoxia-inducing activity of the parental cells was greatly reduced with the depletion of the mitochondrial genome, and recovered with the reconstitution of the genome (Figures 6b and c). To investigate whether the hypoxic-to-normoxic shift induced by the reduction of mitochondrial genome content augments the expression of HMGR, the oxygen condition in the culture of LNCaP cells was increased (30%, 310 μM) to establish an increased intracellular oxygen condition. The expression of HMGR and the phosphorylation of ERK were amplified within 6 h of culture in the enriched oxygen condition (Figure 6d). The study was further refined by the culture of LNρ0-8 in low oxygen environments to exogenously induce a normoxic-to-hypoxic shift in LNρ0-8. The greatly reduced-oxygen condition (0.2%, 2.1 μM), but not 1, 5 or 20%, attenuated the expression of HMGR and the phosphorylation of ERK (Figure 6e), within 6 h of culture in the 0.2% oxygen environments (Figure 6f). The data indicate that hypoxic-to-normoxic or normoxic-to-hypoxic shifts regulate the protein levels of the HMGR enzyme. We observed the hypoxia-inducing activity of advanced PCa cell lines to be low (Figure 6g), an observation that correlates with the oxygen consumption (Figure 6a) and the dysregulation/reduction of the steady state of the mitochondrial genome content in the progression of PCa (Figure 1b).

Endogenous or exogenous induction of the mevalonate pathway in PCa signals the progression of the advanced phenotype *in vitro* and *in vivo*. To verify that exogenous androgens amplify the viability of the early-stages PCa, LNCaP were cultured in androgen-deprived media without (Figure 7a) or with synthetic androgen (R1881) (Figure 7b). Meanwhile, the androgen-deprived media was supplemented with exogenous mevalonate to induce the mevalonate pathway in the absence or presence of exogenous androgen (Figures 7c and d, respectively). Figure 7e demonstrates that exogenous androgens amplify the growth and proliferation of LNCaP in a dose-dependent fashion that is diminished in the presence of exogenous mevalonate. Alternatively, mevalonate alone supports growth in the absence of exogenous androgen (Figures 7c and e). The experiment reveals that exogenous mevalonate induces androgen independence.

In subsequent experiments we evaluated the essentialness of the endogenous mevalonate pathway on the viability of

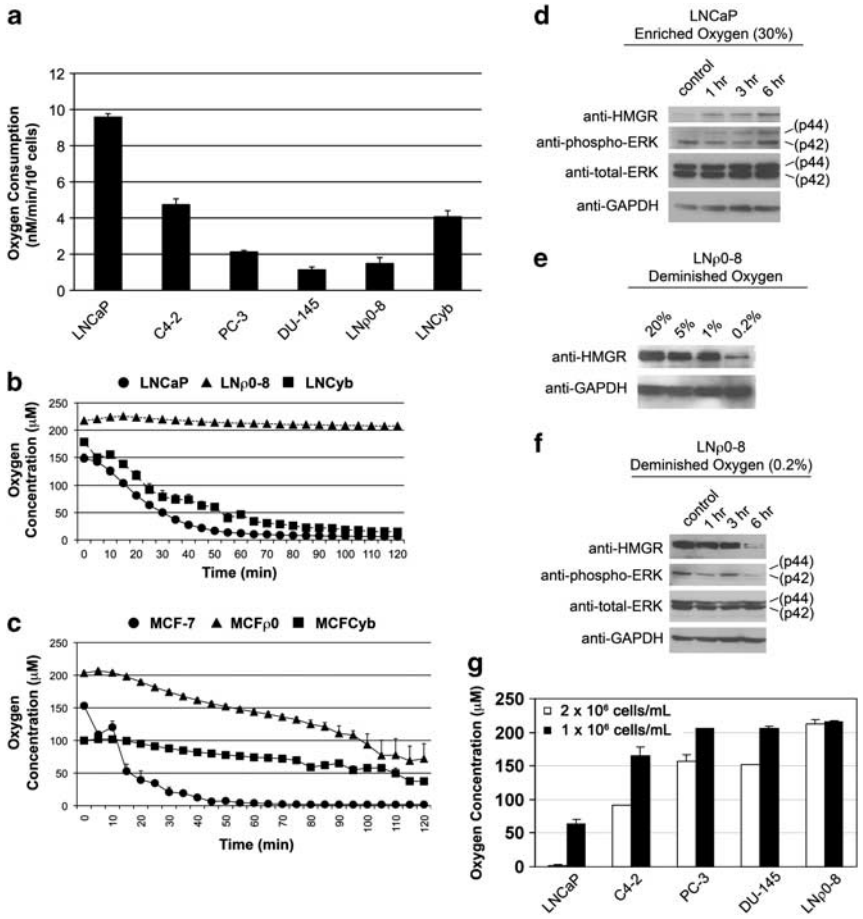

Figure 6 HMGR expression in PCa is enhanced by the hypoxic-to-normoxic change. (**a**) Oxygen consumption rates of the indicated cell lines (1×10^6 cells/ml) (mean ± S.E.) ($n = 3$). (**b** and **c**) Oxygen concentration surrounding the indicated cell lines (2×10^6 cells/ml) (mean ± S.E.) ($n = 3$). (**d**) HMGR and phospho-ERK in total-protein-lysates (30 μg) of LNCaP cultured in 30% oxygen for the indicated time periods. LNCaP were cultured in 20% oxygen as a control. (**e**) HMGR and phospho-ERK in total-protein-lysates (30 μg) of LNρ0-8 seeded (1×10^6 cells/ml) overnight, then cultured 6 h in the indicated oxygen concentration, or (**f**) in 0.2% oxygen for the indicated time periods. LNρ0-8 cells were cultured in 20% oxygen as a control. (**g**) Oxygen concentration surrounding the indicated cell lines (2×10^6 or 1×10^6 cells/ml) (mean ± S.E.) ($n = 3$) after 2 h incubation

PCa that harbor or are devoid of the mitochondrial genome. The viability of LNρ0-8 was significantly diminished in the presence of lovastatin, relative to the parental and mtDNA-KI cells (Figure 7f); the lovastatin-mediated inhibition of the viability of the mtDNA-KO was prevented by mevalonate (Figure 7g). The experiments demonstrate that a reduction of the mitochondrial genome content in PCa is transduced into the advanced phenotype via an endogenous induction of the mevalonate pathway.

LNCaP cells are known to gradually acquire more aggressive growth within *in vitro* and *in vivo* environments.[36,37] In order to investigate, *in vivo*, the role of mevalonate pathway in the shift of LNCaP to more aggressive growth phenotype, we inoculated LNCaP cells into athymic nude mice. Following the development of tumors with diameters of 9–10 mm, mice were randomly assigned to four experimental groups as follows; (1) control, (2) lovastatin, (3) mevalonate and (4) lovastatin and mevalonate. The mean tumor volume for each group was quantified on Day 0 (pre-treatment): 377 ± 105, 336 ± 106, 454 ± 86 and 383 ± 44 (average ± S.D. mm^3). Subsequently, pumps were utilized to systemically deliver either mevalonate (group 3 and group 4) or isotonic saline (group 1 and group 2) into mice, whereas lovastatin was consumed in the diet of mice of group 2 and group 4. Figure 8a demonstrates that the progressive growth of LNCaP (group 1) in mice was significantly reduced with the treatment of lovastatin (group 2); the growth inhibitory effect of lovastatin was reversed with exogenous mevalonate (group 4). Meanwhile, the administration of exogenous mevalonate alone (group 3) slightly but significantly enhanced the growth of LNCaP. These results indicate that the mevalonate pathway is responsible for *in vivo* advanced growth in the xerographic model of PCa.

Discussion

Our collective report demonstrates in PCa that the (1) inhibition of respiration, by reduction of the mitochondrial genome content, shifts cells from a hypoxic-to-normoxic state (2) that attenuates the endogenous proteasomal degradation of the HMGR enzyme; (3) the increase in mevalonate pathway (4) induces the constitutive activation of nuclear-encoded proto-oncogenic Ras (5) that signal for an array of cancer progression signals (Figure 8b). We denote the coherent series of events as the mitoGPS.

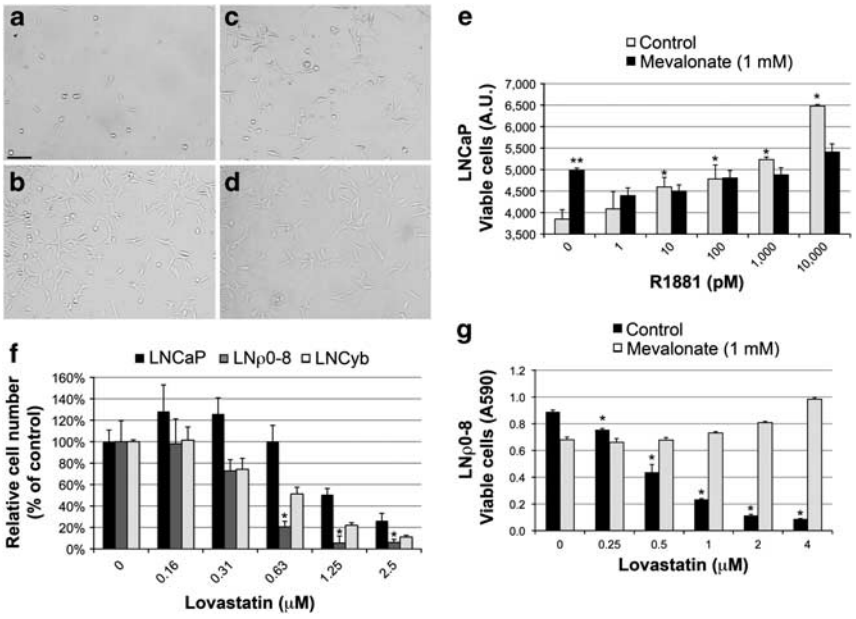

Figure 7 Endogenous or exogenous induction of the mevalonate pathway in PCa signals the progression of the phenotype. Microscopic images of LNCaP cultured 7 days in androgen-deprived media with 5% charcoal stripped bovine serum (no androgen) (**a**) supplemented with synthetic androgen R1881 (**b**), mevalonate (**c**), or mevalonate and R1881 (**d**). Scale bar represents 100 μm. (**e**) Total cell viability was quantified by a calcein assay (arbitrary unit (A.U.) $\pm$ S.E.) ($n=3$). Student's *t*-test compared the control group in the absence or presence of R1881 (*$P<0.01$, except for 10 pM and 100 pM, $P<0.05$), and the control and mevalonate groups cultured in the absence of R1881 (**$P<0.01$). (**f**) Viability of the parental, mtDNA-KO and mtDNA-KI of LNCaP cultured 4 days in the absence or presence of lovastatin ($n=3$). Student's *t*-test compared LNCaP and LNρ0-8 cultured in the same lovastatin concentration (*$P<0.01$). (**g**) Addition of mevalonate to the lovastatin-mediated inhibition of the viability of LNρ0-8. Total cell viability was quantified by a crystal violet assay (average AD590 $\pm$ S.E.) ($n=3$). Student's *t*-test compared the lovastatin groups with the control (no lovastatin, no mevalonate) (*$P<0.001$)

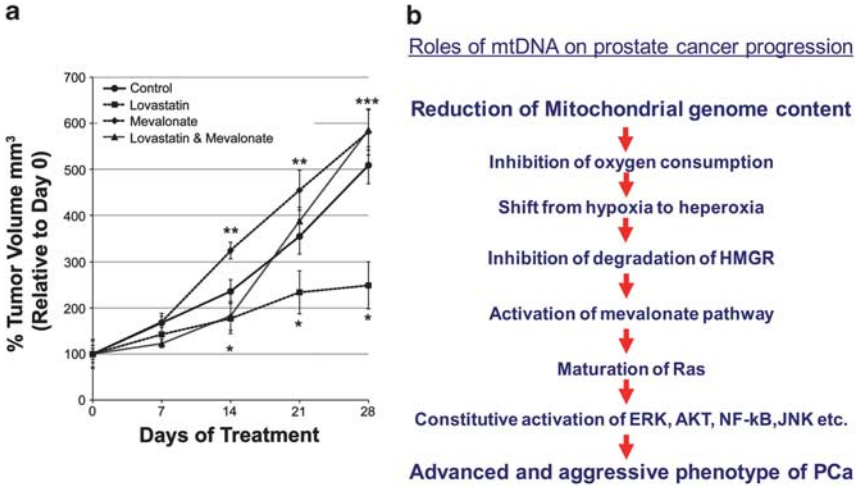

Figure 8 The effect of lovastatin and mevalonate on tumor formations of LNCaP in athymic nude mice. Athymic BALB/c (nu/nu) mice were subcutaneously inoculated with LNCaP. The effect of lovastatin and mevalonate on tumor growth was investigated as described in Materials and Methods. The tumor volumes were measured weekly and calculated. The relative tumor volume was calculated as percent of control $\pm$ S.D. by assuming the rate of each tumor volume on day 0 to be 100% ($n=6$). Student's *t*-test compared the control and lovastatin group showed significance at day 14, 21 and 28 days (*$P<0.01$), and the control and mevalonate groups at day 14 and 21 (**$P<0.01$) and 28 days (***$P<0.02$)

The pathological condition of a deprivation in an adequate oxygen supply to the body is referred to as hypoxia, a condition that is transduced at the molecular level into hypoxia-related signals that allow a cell(s) to adjust to the extracellular environment. We are the first to directly establish the mitochondrion as a direct physiological source of hypoxia in an *in vitro* system. Our results demonstrate that the reduction of the mitochondrial genome content diminishes the hypoxic state of the early stages of PCa and BCa, generating a hypoxic-to-hyperoxic shift in the oxygen content that is transduced into the overexpression of HMGR; subsequently, the induction of the mevalonate pathway activates proto-oncogenic Ras that signals the constitutive and concurrent activation of a diverse array of cancer progression

pathways that advance the disease. Reports indicate that hypoxia inhibits lanosterol demethylase, an oxygen requiring enzyme, and accumulates lanosterol (molecules in cholesterol pathway) and that accumulation of lanosterol induces Insig-mediated degradation of HMGR. Hypoxia also activates HIF-1 to induce expression of insig.[34,35] Whether this pathway is activated in our system is now under investigation. The roles of ROS may not be likely as mtDNA-deficient cells generate reduced superoxide.[38]

With primary PCa composed of a mixture of cells with high or low mitochondrial genome content,[39] cells with high mitochondrial content may generate more hypoxia-induced changes that benefit the growth and maintenance of both groups under high cell density conditions, that is, the primary tumor site. In contrast, we speculate in the initiation of metastasis that the progressive induction of hyperoxia with the reduction of cell-density further enhances the mitoGPS, advancing the phenotype of cancer that harbor a reduced copy-number of the mitochondrial genome. It is plausible that the mitoGPS is a ubiquitous (patho)physiological response to the etiology and/or progression of a broad spectrum of human diseases that are attributed to respiratory incompetent mitochondria in various degenerative diseases (e.g., metabolic syndrome and diabetes). For example, as K-Ras 4A is responsible for aldosterone signaling,[40] the roles of mtDNA changes on hypertension is implicated.

In conclusion, our report has identified an intricate interaction of prospective (mitochondrial and nuclear encoded) markers for the selective penetrance, progression and prognosis of PCa, and potentially a diverse array of respiratory-deficient (e.g., aging) pathologies.

Materials and Methods

Materials. Uridine, sodium pyruvate, rotenone, antimycin A, oligomycin A, mevalonate and FTase-276 were purchased from Sigma-Aldrich (St. Louis, MO, USA).; Lovastatin from A.G. Scientific (San Diego, CA, USA) and ALLN from Fisher Scientific (Pittsburgh, PA, USA).

Cell culture. LNCaP and C4-2 were purchased from UROCOR (Minnetonka, MN, USA); MCF-7, PC-3 and DU-145 were purchased from ATCC (Manassas, VA, USA); and, PrEC was purchased from Lonza (Allendale, NJ, USA). PC-3, DU-145, LNCyb, MCF-7 and MCFCyb were cultured in Dulbecco's modified Eagle medium with a high level of D-glucose (4.5 g/l) and sodium pyruvate (110 mg/l) (Invitrogen, Allendale, NJ, USA), additionally supplemented with 5% fetal calf serum (FCS, Thermo Scientific, Barrington, IL, USA). PrEC was cultured in prostate epithelial cell basal media (PrEBM, Lonza) supplemented with PrEGM SingleQuots: BPE, insulin, HC, GA-1000, retinoic acid, transferrin, T3, epinephrine and rhEGF (no. CC-4177, Lonza). Media for LNρ0-8 and MCFρ0 was additionally supplemented with uridine (50 μg/ml) and sodium pyruvate (100 μg/ml). Media for BCa cells was additionally supplemented with bovine insulin (0.01 mg/ml) (Sigma-Aldrich).

Microdissection. Samples and matched clinical information were obtained from the Division of Urology at McClellan's Memorial Veteran's Hospital (Little Rock, AR, USA). All patient-derived biological specimens were collected and archived under protocols approved by the Human Subjects Committee of the University of Arkansas for Medical Science Institutional Review Board (UAMS IRB no. 55578). In all, 14 PCa patients participated in the study (age ranging from 49–73 years; average 61.7 years). According to the clinical information available, none of these individuals had any medical condition or had any treatment known to affect the prostate. In all, 14 PCa tissues were collected by radical prostatectomy specimens. The cancers ranged from Gleason grade 3 + 3, 3 + 4, 4 + 3, 4 + 4, 4 + 5 or 5 + 4. Fresh specimens were frozen at $-80\,^{\circ}$C and sectioned by cryostat to yield 8 μm sections. Each section was fixed in methanol and stained in Mayer's hematoxylin. Before microdissection, cut sections were dehydrated in ethanol. An expert pathologist selected cancer and normal epithelial regions, and then individual cells were collected by laser microdissection using the Leica AS LMD system (Leica Microsystems, Richmond, IL, USA). The dissected cells were transferred by gravity alone into a microcentrifuge tube placed directly underneath the tissue section. The tube was filled with digestion buffer (20 μl) containing SDS (0.0015%), proteinase K (0.2 mg/ml) and EDTA (4.5 mM) to ensure the isolation of DNA. After incubation (55 $^{\circ}$C for 3 h), the samples were boiled (95 $^{\circ}$C for 10 min) to inactivate proteinase K.

FISH of mitochondrial genome. Alexa-488 dye labeled mtDNA-probes ($\sim$600 bp) were created from six overlapping PCR products ($\sim$3.3 kb in length) that collectively represent the entire human mitochondrial genome were prepared. An equal amount of PCR product from each reaction were combined, and the pooled products were nick-translated and labeled with the Alexa-488 dye as instructed in the ARES Alexa-488 DNA Labeling Kit (Invitrogen).

Cells were seeded (60% confluence) on submerged cover slips. To counter stain the mitochondria, cell cultures were incubated (20 min at 37 $^{\circ}$C) in MitoTracker Red dye (300 nM) (Molecular Probes). Cells were then washed in PBS, and fixed (10 min at 37 $^{\circ}$C) in 4% formaldehyde (Ted Pella, Redding, CA, USA). Fixed cells were washed in PBS, and permeabilized (5 min at 25 $^{\circ}$C) in 0.1% Triton X-100 (Sigma-Aldrich). Cells were then washed in PBS, and treated (90 min at 37 $^{\circ}$C) with 0.1 mg/ml DNase-free RNase (Roche Diagnostics, Indianapolis, IN, USA). Cells were then washed with PBS; meanwhile, the mtDNA probes (0.5 ng/ml) were denatured (10 min at 74 $^{\circ}$C) in formamide (50%), dextran sulfate (10%) and 2 $\times$ saline sodium citrate (SSC) buffer. Cover slips were mounted with denatured probes (15 μl) onto pre-warmed slides (74 $^{\circ}$C). Cover slips and the mtDNA probes were sealed to the slides with rubber cement and left overnight in a dark humidified chamber (37 $^{\circ}$C) to hybridize. After hybridization the cover slips were removed from the slides and washed in 2 $\times$ SSC buffer at 25 $^{\circ}$C, followed by sequential washes in 2 $\times$ SSC and 0.5 $\times$ SSC buffer at 40 $^{\circ}$C. Cover slips were then rinsed in PBS and mounted to slides by ProLong antifade reagent with or without 4′, 6-diamidino-2-phenylindole dihydrochloride (DAPI) (Invitrogen).

Wide field fluorescence microscopy. Wide field microscopy imaging was performed with a Zeiss Axioskop 40 microscope (Carl Zeiss, Thornwood, NY, USA) fitted with a $\times$ 40/0.75 NA objective. Images were captured with a Zeiss AxioCam MRm camera, and collected using AXIOVISION software (Carl Zeiss). Matched image sets were mapped to a common linear gray-scale range. Images were prepared for publication with ADOBE PHOTOSHOP software (Adobe Systems, San Jose, CA, USA).

Spinning disk fluorescence microscopy. Confocal imaging was performed with a Zeiss Axiovert 200 M microscope (Carl Zeiss) fitted with a $\times$ 100/1.40 NA objective and a CARV II spinning disk confocal accessory (BD Bioimaging, RockVille, MA, USA) mounted to the sideport of the microscope. Images were captured with a Retiga EXi camera (QImaging, Surey, BC, Canada). The microscope was operated in multitrack configuration with alternative excitation, as controlled with IVISION MAC (BioVision Technologies, Exton, PA, USA). Image stacks were collected through the entire cell depth, and then compressed into a single plane using maximum intensity projection and IVISION (Atlanta, GA, USA) software. When noted, a single z-slice (plane) was captured using a $\times$ 100/1.40 NA objective. Matched image sets were mapped to a common linear gray-scale range. Images were prepared for publication with ADOBE PHOTOSHOP software (Adobe Systems).

SDS-PAGE and western blotting. Cells were lysed in radioimmunoprecipitation assay buffer supplemented with DTT (0.5 mM), and protease and phosphatase inhibitors (100 $\times$ Halt protease and phosphate inhibitor cocktail, no. 1861281, Thermo Scientific). Cytosolic extracts were isolated by centrifugation (12 000 *g* for 15 min at 4 $^{\circ}$C), and the protein concentration was determined by a protein assay (Bio-Rad Protein Assay, Bio-Rad, Hercules, CA, USA). Total-protein lysates were suspended in reducing SDS gel-loading buffer, denatured (95 $^{\circ}$C for 5 min) and subjected to electrophorectic separation in polyacrylamide slab gels in the presence of SDS (i.e., SDS-PAGE), and then transferred to immobilon-P membrane (Millipore, Bellelica, MA, USA). After a wash in Tris Buffered Solution (TBS), the membrane was incubated overnight (4 $^{\circ}$C) in primary antibody diluted (1 : 1000) in bovine serum albumin (5% BSA, Sigma-Aldrich). Antibodies utilized in the current study are as follows: rabbit anti-phospho ERK(T202/Y204) (no. 9101), rabbit anti-total ERK (no. 9102), rabbit anti-phospho Akt(Ser473) (no. 9271), rabbit anti-total Akt (no. 9272), rabbit anti-β-actin (no. 4967, Cell Signaling, Beverly, MA, USA),

mouse anti-total Ras (clone RAS10, no. 05-516, Millipore), rabbit anti-H-Ras (C-20, no. sc-520), rabbit anti-K-Ras 4A (C-17, no. sc-522), rabbit anti-K-Ras 4B (C-19, no. sc-521), rabbit anti-N-Ras (C-20, no. sc-519, Santa Cruz Biotechnology, Santa Cruz, CA, USA), rabbit anti-total DAB2IP (no. A302-439A, Bethyl Laboratories, Montgomery, TX, USA), rabbit anti-HMGR reductase (no. 07-457, Millipore), and mouse anti-GAPDH (no. MAB374, Millipore). The membrane was then washed in TBS, and incubated (1 h at RT) with HRP-linked anti-mouse IgG or anti-rabbit IgG diluted (1 : 10 000) in 5% BSA-TBS (no. 7074 and no. 7076, respectively, Cell Signaling). The membrane was then washed in TBS, and analyzed with ECL Plus (GE Healthcare Bio-Sciences AB, Uppsala, Sweden) by autoradiography film.

Ras activation (Pull Down) assay. Activated (GTP-bound) Ras was pulled down from total-protein lysates of cell cultures by a Ras Activation Assay kit (Kit no. 17-218, Millipore). Briefly, an agarose-bound GST fusion protein corresponding to the RBD (residues 1–149) of human c-Raf was utilized to bind and precipitate GTP-bound Ras from total-protein lysates. As a negative control, before pull-down an aliquot of total protein lysate was pre-loaded with GDP to deactivate (GTP-bound) Ras to the GDP-bound state. As a positive control, before pull-down an aliquot of total protein lysate was pre-loaded with nonhydrolyzable GTPγS to active (GDP-bound) Ras to the GTP-bound state. Protein levels of pulled down Ras in samples were analyzed by SDS-PAGE and western blot.

Genomic sequencing of K-RAS. A DNA extraction kit (ZR Genomic DNA II Kit, Zymo Research, Irvine, CA, USA) was used to prepare genomic DNA. Primers were custom synthesized (Integrated DNA Technologies, Coralville, IA, USA) to amplify the *K-RAS* gene in exon 1 (codon 12 and 163 bp) and in exon 2 (codon 61, 133 bp): exon 1: exon 1 (sense 5′-GGCCTGCTGAAAATGACTGAA-3′ and anti-sense 5′-GGTCCTGCACCAGTAATATGC-3′) and exon 2 (sense 5′-CAGGATTCC TACAGGAAGCAAGTA-3′ and anti-sense 5′-CACAAAGAAAGCCCTCCCCA-3′). PCR was carried out with La Taq DNA polymerase (TaKaRa, Shiga, Japan): 94 °C for 1 min; 30 sequential cycles of 94 °C for 15 s, 55 °C (exon 1) or 60 °C (exon 2) for 30 s, and 72 °C for 10 s; with a final elongation at 72 °C for 1 min. PCR products were loaded onto an agarose gel (2%) to confirm a single target band. The target band was cut out and purified using the Wizard PCR Preps DNA Purification System (Promega, Madison, WI, USA), then subjected to direct sequencing with a 3100 Genetic Analyzer (Applied Biosystems, Carlsbad, CA, USA; UAMS DNA Sequencing Core Facility, Little Rock, AR, USA).

Measurement of oxygen consumption. Cells (1×10^6) were suspended in 1 ml of culture medium pre-equilibrated to 20% oxygen and then placed in a sealed respiration chamber equipped with a thermostat control and a micro-stirring device (Oxytherm, Hansatech Instrument, King's Lynn, Norfolk, UK). The oxygen contents in the starting medium were normalized assuming an O_2 concentration of 217 μM in air-saturated medium at 37 °C ($n = 3$).

Oxygen concentration measurements by OxoPlate. The OxoPlate OP96U (PreSens) contains oxygen-sensitive, polystyrene particles PSLi-Pt-1 (Opto-Sense). Sulforhodamin is covalently attached to these particles as reference dye, and a platinum porphin is incorporated as indicator dye. The sensor has a thickness of about 10 μm and is fixed at the bottom of each well of a 96-round bottom microtiter plate (Greiner, Monroe, NC, USA). Cells (200 μl) were added to each well at the indicated cell density. Wells containing oxygen-free water (*cal 0*) and air-saturated water (*cal 100*) served as standards. Oxygen-free water was prepared by dissolving sodium sulfite (1%) in water; in the wells, the oxygen-free water was overlaid with mineral oil (50 μl) to prevent the diffusion of oxygen into the wells. The oxygen concentration (fluorescence) in each well was quantified for 3 h in 5-min intervals, as measured in a dual kinetic mode (Synergy HT, BIO-TEK, Einooski, VT, USA): filter pair 1 (544/650 nm) detects fluorescence of the indicator dye; the second measures fluorescence (544/590 nm) of the reference dye ($n = 3$).

Calculation of oxygen concentration. The relationship between fluorescence and dissolved oxygen is nonlinear, as described by the Stern–Volmer equation:

$$\frac{I_R}{I_{R,0}} = \frac{1}{1 + K_{sv}[O_2]}$$

where, $I_{R,0}$ is the fluorescence intensity ratio in the absence of oxygen; I_R is the fluorescence intensity ratio at the oxygen concentration [O_2], and K_{SV} the Stern–Volmer parameter. Intensity ratios I_R are calculated for each individual well by dividing the intensity of the indicator dye by the intensity of the reference dye. A two-point calibration is sufficient: $[O_2] = 0$ and at $[O_2] = [O_2]^*$, where $[O_2]^*$ is the saturation concentration.

Oxygen concentration as a percentage of air saturation was calculated for each well, as follows:

$$pO_2 = 100 \times \left(\frac{K_O}{I_R} - 1\right) / \left(\frac{K_O}{K_{100}} - 1\right)$$

where the constant K_0 is defined as I_R of well filled with *cal 0*. Analogously, K_{100} is defined as I_R of well filled with *cal 100*.

Culture of cells in high or low oxygen condition. LNCaP (0.25×10^6 cells) and LNρ0-8 (1×10^6 cells) were seeded in a 6-cm culture dish overnight in a humidified atmosphere of 5% CO_2 in an incubator. Increased and reduced oxygen incubations were carried out in a C-chamber (no. C-174, BioSpherix, Lacona, NY, USA), regulated by a PRO-OX 110 oxygen controller (Biospherix) to establish the indicated oxygen concentrations. (DMEM + 5% FCS, 50 mM HEPES) and Additional Gases (nexAir: Nitrogen Liquid Medical Grade LS180 ltrs 22psi (no. LQ NI-NF-LS180) (Santa Cruiz, CA) and Oxygen Medical Grade 200 + cft (no. HP OX-USP-2)).

QRT-PCR of the mitochondrial genome content. The mitochondrial genome content of individual cells was quantified by QRT-PCR as previously described.[39]

RT-PCR of RAS. Total-RNA was isolated with a Qiagen RNA-Plus Mini Easy kit (no. 74134, Qiagen , Valencia, CA, USA), subjected (2 μg) to a gDNA eliminator spin column, primed with oligo $(dT)_{18-20}$ (Invitrogen), and reverse transcribed by Superscipt III Reverse Transcriptase (Invitrogen). Primers were custom synthesized (Integrated DNA Technologies) to amplify the cDNA for H-RAS (111 bp), K-RAS 4A (560 bp), K-RAS 4B (711 bp), N-RAS (682 bp), HMGR (280 bp) and GAPDH (89 bp): H-RAS (sense 5′-ATGACGGAATATAAGCTGGT-3′ and anti-sense 5′-CTCTATAGTGGGGTC GTATT-3′); K-RAS 4A (sense 5′-GAGAGAGGCC TGCTGAAAATG-3′ and anti-sense 5′-ACACAGCCAGGAGTCTTTTCTTC-3′); K-RAS 4B (sense 5′-AGCGCGGCGCAGGCACTGAA-3′ and anti-sense 5′-TTAGTGTAATGTACAAAAATTACCA-3′); N-RAS (sense 5′-CTGTGGTCCTA AATCT;GTCC-3′ and anti-sense 5′-CAGTGCAGCTTGAAAGTG -3′); HMGR (sense 5′-TGCTGCTTTGGCTGTATGTC-3′ and anti-sense 5′-TGAGCGTGAACAA GAACCAG-3′); GAPDH (sense 5′-GGTGGTCTCCTCTGACTTCAA-3′ and anti-sense 5′-AGCTTGACAAAAGTGGTCGTTG-3′). The entire coding sequence of GAPDH cDNA was amplified as a control. Ex Taq (TaKaRa) was used for the amplification of Ras cDNA or HMGR cDNA from total-cDNA, 50 ng or 200 ng, respectively. The PCR cycle to amplify target cDNA is as follows: 94 °C for 1 min, followed by 20 (Ras) or 35 (HMGR/GAPDH) sequential cycles of 94 °C for 15 s, the denoted annealing temperature (as follows) for 1 min, and 72 °C for 1 min; with a final elongation at 72 °C for 5 min. Annealing temperatures for primers: H-RAS (56 °C); K-RAS 4A (50 °C); K-RAS 4B (56 °C); N-Ras (58 °C); HMGR (58 °C); GAPDH (58 °C). PCR products were separated in agarose gels (RAS cDNA, except H-RAS 1.2%; HMGR 1.5%; H-RAS and GAPDH 2%) supplemented with ethidium bromide (1 : 20 000), and then visualized by a UV transilluminator (UVP, Upland, CA, USA).

K-RAS siRNA. Stealth siRNA duplex oligonucleotides against K-RAS (KRASHSS180200) were custom synthesized (Invitrogen). The sequences were as follows: (RNA)-UGUGGUAGUUGGAGCUGGUGGCGUA and UACGCCACCAG CUCCAACUACCACA. LNρ0-8, seeded at 30% confluence in a 25 cm^2 culture flask overnight, were transfected with 100 ng of K-RAS siRNA or random siRNA (no. 12935-200 (Low GC), Invitrogen), using 10 μg of Lipofectamine 2000 (Invitrogen) as directed by the manufacturer's protocol. Protein lysates were collected 72 h post-transfection.

Immunocytochemistry of anti-total-Ras. Cells were seeded (60% confluence) on submerged cover slips. Cover slips were washed with PBS, then fixed and permeabilized as previously described. Permeabilized cells were blocked (1 h) in 5% normal goat serum (Vector Laboratories, Burlingame, CA, USA). Ras was probed with anti-total-Ras diluted (1 : 1000) in blocking solution overnight at 4 °C, and then washed in PBS. Alexa-488 anti-mouse IgG (Invitrogen) was applied (1 h at RT) to the cover slips (1 : 500) in blocking solution. Cover slips were then

washed in PBS and mounted on top of ProLong antifade reagent with or without DAPI (Molecular Probes).

Detection of cell viability by microscopic analysis. Cells were cultured (2000 cells per 200 μl/well) in a 96 well flat-bottomed microtiter plate. Phase-contrast image analysis was conducted by a Fisher Scientific MICROMASTER INVERTED microscope fitted with a $\times$ 40/1.5 NA objective. Image were collected and prepared for publication with ADOBE PHOTOSHOP software (Adobe Systems).

Assay of cell viability by calcein. Cells were cultured (2000 cells per 200 μl/well) in a 96-well flat-bottomed microtiter plate (Fisher Scientific) that was centrifuged (250 *g* for 5 min at 4 °C) to avoid the loss of cells in the staining process. The media was removed (170 μl) and PBS (100 μl) was added to each well, followed by the addition of Calcein-AM working solution (10 μl) (EMD Chemicals, Philadelphia, PA, USA). The plate was then incubated (37 °C for 1 h) in a CO_2 incubator. The fluorescence of the samples was measured by a microtiter plate spectrophotometer (BioTek Synergy HT plate reader, BIO-TEK) (excitation 485 $\pm$ 10 nm and emission 520 $\pm$ 10 nm). All cultures were performed in triplicate ($n = 3$) and the mean was displayed as an arbitrary unit (A.U.) $\pm$ S.E.

Assay of cell viability by crystal violet. Cells were cultured in a 96-well flat-bottomed microtiter plate (2000 cells per 200 μl/well). Subsequently, the supernatants were discarded and the remaining viable adherent cells were stained (5 min) with crystal violet (0.2%) in 20% ethanol. The microtiter plate was then rinsed with water and solubilization solution (100 μl of H_2O : methanol : ethanol = 5 : 1 : 4) was added to each well. The absorbance of each well was read at 590 nm with a microtiter plate spectrophotometer. All cultures were performed in triplicate ($n = 3$) and results were expressed by mean $\pm$ S.E.

Animal studies. Athymic BALB/c (nu/nu) mice (Clea Japan Inc., Tokyo, Japan), 4 weeks of age, were subcutaneously inoculated with LNCaP cells (5.0×10^6 cells per 50 μl of medium). Following the development of tumors with diameters of 7–8 mm, 24 mice were randomly assigned to four experimental groups as follows: group 1, isotonic saline (control) (6 mice); group 2, lovastatin (5 mg/kg/day) (6 mice); group 3, mevalonate (36 μmol/day) (6 mice); and group 4, lovastatin (5 mg/kg/day) and mevalonate (36 μmol/day) (6 mice). 200-μl miniosmotic pumps (flow rate 0.25 μl/h, 28-days pumping life) (Alzet Corp., Palo Alto, CA, USA) were subcutaneously implanted in the intrascapular area of all mice at Day 0. Pumps delivered either mevalonate (group 2 and group 4) or isotonic saline (group 1 and group 3) from day 0 to day 28. The diet contain an additional lovastatin were fed to mice of group 2 and group 4 from day 0 to day 28. The tumor volumes were measured weekly for 4 weeks and calculated by using the following formula: volume (a rotational ellipsoid) = $M1 \times M2^2 \times 0.5236$, where M1 = the long axis and M2 = the short axis. The relative tumor volume was calculated by assuming the rate of each tumor volume on day 0 to be 100%. Experiments in each group were performed in six plicate and results were expressed by mean $\pm$ S.D. All the aspects of the experimental design and procedure were reviewed and approved by the institutional ethics and animal welfare committees of The Hyogo University of Health Sciences (2009-19-1).

Conflict of Interest

The authors declare no conflict of interest.

Acknowledgements. This work was supported by Taiho Pharmaceutical Co. Ltd, State of Arkansas Tobacco Settlement, NIH grant CA100846 to MH and DOD PCRP Prostate Cancer Training Award to CCC. We thank Drs. Kiyoshi Kita, Michael Douglas and Yung C Lin for reviewing the manuscript. We also are thankful for the technical assistance of Drs. Takatsugu Mizumachi, Dwight Pierce, Kim Light and Brian Storrie.

1. American Cancer Society. *Cancer Facts & Figures*. ACS: Atlanta, GA, 2009.
2. Anderson S, Bankier AT, Barrell BG, de Bruijn MH, Coulson AR, Drouin J *et al.* Sequence and organization of the human mitochondrial genome. *Nature* 1981; **290**: 457–465.
3. Carew JS, Huang P. Mitochondrial defects in cancer. *Molecular Cancer* 2002; **1**: 1–12.
4. Ishikawa K, Takenaga K, Akimoto M, Koshikawa N, Yamaguchi A, Imanishi H *et al.* ROS-generating mitochondrial DNA mutations can regulate tumor cell metastasis. *Science* 2008; **320**: 661–664.
5. Chen JZ, Gokden N, Greene GF, Mukunyadzi P, Kadlubar FF. Extensive somatic mitochondrial mutations in primary prostate cancer using laser capture microdissection. *Cancer Res* 2002; **62**: 6470–6474.
6. Barthelemy C, de Baulny HO, Lombes A. D-loop mutations in mitochondrial DNA: link with mitochondrial DNA depletion? *Human Genetics* 2002; **110**: 479–487.
7. Chandel NS, Schumacker PT. Cells depleted of mitochondrial DNA (rho0) yield insight into physiological mechanisms. *FEBS Letters* 1999; **454**: 173–176.
8. Higuchi M, Aggarwal BB, Yeh ET. Activation of CPP32-like protease in tumor necrosis factor-induced apoptosis is dependent on mitochondrial function. *J Clin Invest* 1997; **99**: 1751–1758.
9. Higuchi M, Kudo T, Suzuki S, Evans TT, Sasaki R, Wada Y *et al.* Mitochondrial DNA determines androgen dependence in prostate cancer cell lines. *Oncogene* 2006; **25**: 1437–1445.
10. Naito A, Cook CC, Mizumachi T, Wang M, Xie CH, Evans TT *et al.* Progressive tumor features accompany epithelial-mesenchymal transition induced in mitochondrial DNA-depleted cells. *Cancer Science* 2008; **99**: 1584–1588.
11. Xie CH, Naito A, Mizumachi T, Evans TT, Douglas MG, Cooney CA *et al.* Mitochondrial regulation of cancer associated nuclear DNA methylation. *Biochem Biophys Res Commun* 2007; **364**: 656–661.
12. Nishimura G, Proske RJ, Doyama H, Higuchi M. Regulation of apoptosis by respiration: cytochrome c release by respiratory substrates. *FEBS Lett* 2001; **505**: 399–404.
13. Suzuki S, Naito A, Asano T, Evans T, Reddy S, Higuchi M. Constitutive Activation of AKT Pathway Inhibits TNF-induced Apoptosis in Mitochondrial DNA-Deficient human myelogenous leukemia ML-1a. *Cancer Lett* 2008; **268**: 31–37.
14. McCubrey JA, Steelman LS, Chappell WH, Abrams SL, Wong EW, Chang F *et al.* Roles of the Raf/MEK/ERK pathway in cell growth, malignant transformation and drug resistance. *Biochem Biophys Acta* 2007; **1773**: 1263–1284.
15. Gioeli D, Mandell JW, Petroni GR, Frierson Jr HF, Weber MJ. Activation of mitogen-activated protein kinase associated with prostate cancer progression. *Cancer Res* 1999; **59**: 279–284.
16. Gao H, Ouyang X, Banach-Petrosky WA, Gerald WL, Shen MM, Abate-Shen C. Combinatorial activities of Akt and B-Raf/Erk signaling in a mouse model of androgen-independent prostate cancer. *Proc Natl Acad Sci USA* 2006; **103**: 14477–14482.
17. Bakin RE, Gioeli D, Bissonette EA, Weber MJ. Attenuation of Ras signaling restores androgen sensitivity to hormone-refractory C4-2 prostate cancer cells. *Cancer Res* 2003; **63**: 1975–80.
18. Horoszewicz JS, Leong SS, Chu TM, Wajsman ZL, Friedman M, Papsidero L *et al.* The LNCaP cell line – a new model for studies on human prostatic carcinoma. *Prog Clin Biol Res* 1980; **37**: 115–132.
19. Wu HC, Hsieh JT, Gleave ME, Brown NM, Pathak S, Chung LW. Derivation of androgen-independent human LNCaP prostatic cancer cell sublines: role of bone stromal cells. *Int J Cancer* 1994; **57**: 406–412.
20. Kaighn ME, Narayan KS, Ohnuki Y, Lechner JF, Jones LW. Establishment and characterization of a human prostatic carcinoma cell line (PC-3). *Invest Urol* 1979; **17**: 16–23.
21. Stone KR, Mickey DD, Wunderli H, Mickey GH, Paulson DF. Isolation of a human prostate carcinoma cell line (DU 145). *Int J Cancer* 1978; **21**: 274–281.
22. Soule HD, Vazguez J, Long A, Albert S, Brennan M. A human cell line from a pleural effusion derived from a breast carcinoma. *J Natl Cancer Inst* 1973; **51**: 1409–1416.
23. Zhang XF, Settleman J, Kyriakis JM, Takeuchi-Suzuki E, Elledge SJ, Marshall MS *et al.* Normal and oncogenic p21ras proteins bind to the amino-terminal regulatory domain of c-Raf-1. *Nature* 1993; **364**: 308–313.
24. Minden A, Lin A, McMahon M, Lange-Carter C, Derijard B, Davis RJ *et al.* Differential activation of ERK and JNK mitogen-activated protein kinases by Raf-1 and MEKK. *Science* 1994; **266**: 1719–1723.
25. Rodriguez-Viciana P, Warne PH, Dhand R, Vanhaesebroeck B, Gout I, Fry MJ *et al.* Phosphatidylinositol-3-OH kinase as a direct target of Ras. *Nature* 1994; **370**: 527–532.
26. Dote H, Toyooka S, Tsukuda K, Yano M, Ouchida M, Doihara H *et al.* Aberrant promoter methylation in human DAB2 interactive protein (hDAB2IP) gene in breast cancer. *Clin Cancer Res* 2004; **10**: 2082–2089.
27. Min J, Zaslavsky A, Fedele G, McLaughlin SK, Reczek EE, De Raedt T *et al.* An oncogene-tumor suppressor cascade drives metastatic prostate cancer by coordinately activating Ras and nuclear factor-kappaB. *Nat Med* 2010; **16**: 286–294.
28. Jancik S, Drabek J, Radzioch D, Hajduch M. Clinical relevance of KRAS in human cancers. *J Biomed Biotechnol* 2010; **2010**: 150960.
29. Konstantinopoulos PA, Karamouzis MV, AG. Post-translational modifications and regulation of the RAS superfamily of GTPases as anticancer targets. Nature Reviews. *Drug Discovery* 2007; **6**: 541–555.
30. Willumsen BM, Christensen A, Hubbert NL, Papageorge AG, Lowy DR. The p21 ras C-terminus is required for transformation and membrane association. *Nature* 1984; **310**: 583–586.

31. Manne V, Roberts D, Tobin A, O'Rourke E, De Virgilio M, Meyers C *et al.* Identification and preliminary characterization of protein-cysteine farnesyltransferase. *Proc Natl Acad Sci USA* 1990; **87**: 7541–7545.
32. Reiss Y, Goldstein JL, Seabra MC, Casey PJ, Brown MS. Inhibition of purified p21ras farnesyl:protein transferase by Cys-AAX tetrapeptides. *Cell* 1990; **62**: 81–88.
33. Chang TY, Chang CC, Ohgami N, Yamauchi Y. Cholesterol sensing, trafficking, and esterification. *Annu Rev Cell Dev Biol* 2006; **22**: 129–157.
34. Song BL, Javitt NB, DeBose-Boyd RA. Insig-mediated degradation of HMG CoA reductase stimulated by lanosterol, an intermediate in the synthesis of cholesterol. *Cell Metabolism* 2005; **1**: 179–189.
35. Nguyen AD, McDonald JG, Bruick RK, DeBose-Boyd RA. Hypoxia stimulates degradation of 3-hydroxy-3-methylglutaryl-coenzyme A reductase through accumulation of lanosterol and hypoxia-inducible factor-mediated induction of insigs. *J Biol Chem* 2007; **282**: 27436–27446.
36. Igawa T, Lin FF, Lee MS, Karan D, Batra SK, Lin MF. Establishment and characterization of androgen-independent human prostate cancer LNCaP cell model. *Prostate* 2002; **50**: 222–235.
37. Thalmann GN, Sikes RA, Wu TT, Degeorges A, Chang SM, Ozen M *et al.* LNCaP progression model of human prostate cancer: androgen-independence and osseous metastasis. *Prostate* 2000; **44**: 91–103.
38. Higuchi M, Manna SK, Sasaki R, Aggarwal BB. Regulation of the activation of nuclear factor kappaB by mitochondrial respiratory function: evidence for the reactive oxygen species-dependent and -independent pathways. *Antioxidants Redox Signaling* 2002; **4**: 945–955.
39. Mizumachi T, Muskhelishvili L, Naito A, Furusawa J, Fan CY, Siegel ER *et al.* Increased distributional variance of mitochondrial DNA content associated with prostate cancer cells as compared with normal prostate cells. *Prostate* 2008; **68**: 408–417.
40. Terada Y, Kobayashi T, Kuwana H, Tanaka H, Inoshita S, Kuwahara M *et al.* Aldosterone stimulates proliferation of mesangial cells by activating mitogen-activated protein kinase 1/2, cyclin D1, and cyclin A. *J Am Soc Nephrol* 2005; **16**: 2296–2305.